Optical Second Harmonic Generation in Plasmonic Nanostructures: From Fundamental Principles to Advanced Applications

Jérémy Butet,*,† Pierre-François Brevet,‡ and Olivier J. F. Martin†

†Nanophotonics and Metrology Laboratory (NAM), Swiss Federal Institute of Technology Lausanne (EPFL), 1015 Lausanne, Switzerland and ‡Institut Lumière Matière, UMR CNRS 5306, Université Claude Bernard Lyon, 69622 Cedex, Villeurbanne, France

ABSTRACT Plasmonics has emerged as an important research field in nanoscience and nanotechnology. Recently, significant attention has been devoted to the observation and the understanding of nonlinear optical processes in plasmonic nanostructures, giving rise to the new research field called nonlinear plasmonics. This review provides a comprehensive insight into the physical mechanisms of one of these nonlinear optical processes, namely, second harmonic generation (SHG), with an emphasis on the main differences with the linear response of plasmonic nanostructures. The main applications, ranging from the nonlinear optical characterization of nanostructure shapes to the optimization of laser beams at the nanoscale, are summarized and discussed. Future directions and developments, made possible by the unique combination of SHG surface sensitivity and field enhancements associated with surface plasmon resonances, are also addressed.

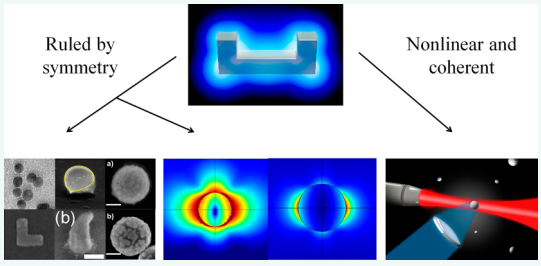

KEYWORDS: plasmonics · nonlinear optics · symmetry · second harmonic generation · sensing · optical characterization · nanoantenna · nanostructures · optics of metals

Nonlinear optics (NLO) was born only 1 year after the invention of the laser:[1] in 1961, Franken *et al.* reported the first observation of a nonlinear optical process, namely, the generation of second harmonic light (SHG) from a quartz crystal pumped by a ruby laser beam.[2] Since this first observation, a lot of work has been devoted to the development of new theoretical models and experimental methods for NLO.[3,4] These efforts have led to the 1981 Nobel Prize in physics shared by Bloembergen and Schawlow for their contributions to the development of laser spectroscopy. The advances in NLO have been shaped by the evolution of modern optics, and nonlinear optical processes have been investigated in a huge variety of optical devices, ranging from optical fibers to photonic crystals, in addition to nonlinear crystals specifically designed for NLO. During the past decades, nanophotonics and, more particularly, plasmonics have emerged as vivid fields of research, triggered by the promises of new applications and the support of recent technology developments.[5] Indeed, plasmonic nanostructures have the unique ability to localize electromagnetic fields in nanoscale volumes, far beyond the limit established by diffraction, permitting control of the properties of light at dimensions much smaller than its wavelength.[6,7] The optical properties of plasmonic nanostructures are intimately linked to the physical phenomenon called localized surface plasmon resonances (LSPR), which corresponds to the collective oscillations of the conduction electrons over a static ionic background. The combination of the strong near-field intensity obtained with plasmonic systems and the intrinsic nonlinearities of metals readily results in efficient nonlinear optical processes, which have given rise to the new research field of nonlinear plasmonics.[8] Various nonlinear optical processes, including SHG,[9−12] multiphoton

* Address correspondence to jeremy.butet@epfl.ch.

Received for review July 15, 2015 and accepted October 16, 2015.

Published online October 16, 2015
10.1021/acsnano.5b04373

excited luminescence,[13−15] third harmonic generation (THG),[16−20] or four-wave mixing (FWM),[21,22] have been observed in plasmonic nanostructures, underlining their great potential to design advanced nonlinear nanosources of light and to manipulate light at small scales. Nonlinear plasmonics is obviously at the frontier between NLO and plasmonics, and every progress made in the field requires merging ideas and paradigms from these two domains, as well as the development of new specific approaches. The large variety of concepts discussed in nonlinear plasmonics, derived from either NLO or plasmonics, not only enriches the domain but also makes it more complex. The aim of this review is to provide the reader with a comprehensive discussion of SHG in plasmonic nanostructures. Differently from the broader scope of the review recently published by Kauranen and Zayats,[8] we choose here to focus on a single nonlinear optical process, namely, SHG, and give an in-depth overview of its basic features and applications. As opposed to odd nonlinear processes involving odd powers of the fundamental field amplitudes and sensitive to volume effects, SHG is appealing due to its sensitivity to centrosymmetry, providing a unique tool to investigate metallic nanostructures.

This review is organized as sketched in Figure 1. The origin of SHG from plasmonic nanostructures is discussed first, providing a clear insight into the physical mechanisms at the origin of SHG in plasmonic nanostructures and emphasizing the main differences with the linear response. The aim of this review is not to report all the details of the microscopic description of SHG but rather to give a clear view on the specificity of SHG and its applications, ranging from nonlinear optical characterization of plasmonic nanostructures to the optimization of laser beams at the nanoscale. Although the discussion is kept at a basic level, the reader is provided with all the tools and concepts required for understanding the peculiarity of SHG in plasmonic nanostructures. This review should be useful for those entering this field of research, experts in NLO interested in plasmonics for the design of new optical devices, or biologists

VOCABULARY: second harmonic generation (SHG), the nonlinear optical process whereby two photons at the fundamental frequency are converted into one photon at twice that frequency; **hyper-Rayleigh scattering (HRS),** corresponds to incoherent SHG and is often used for the measurement of the second-order nonlinear "cross section", also termed "first hyperpolarizability", of nano-objects in solution, with its incoherent nature stemming from the random orientation of the nano-objects, whether they are nanoparticles or molecules, induced by the Brownian motion; **centrosymmetry,** in point group theory, an object is centrosymmetric if its properties at point (x, y, z) and $(-x, -y, -z)$ are identical irrespective of the (x, y, z) point; **nonlinear polarization,** the electromagnetic source of the nonlinear wave produced as a response of the medium to the incident electromagnetic field, scaling with the nonlinear susceptibility which describes the medium; **nonlinear susceptibility,** a tensor describing the nonlinear response of a material to an exciting incident field; **retardation effects,** effects observed due to the spatial variation of the electromagnetic field over a wavelength, manifesting themselves when the illuminated nanostructures have sizes non-negligible as compared to the wavelength; **multipolar radiation,** the intrinsic nature of the emission from a finite size electromagnetic source is multipolar, *i.e.*, includes dipole, quadrupole, octupole,... orders—in most physical problems, for sources with sizes much smaller than the wavelength of the incident light, the electric dipole order largely dominates over higher orders;

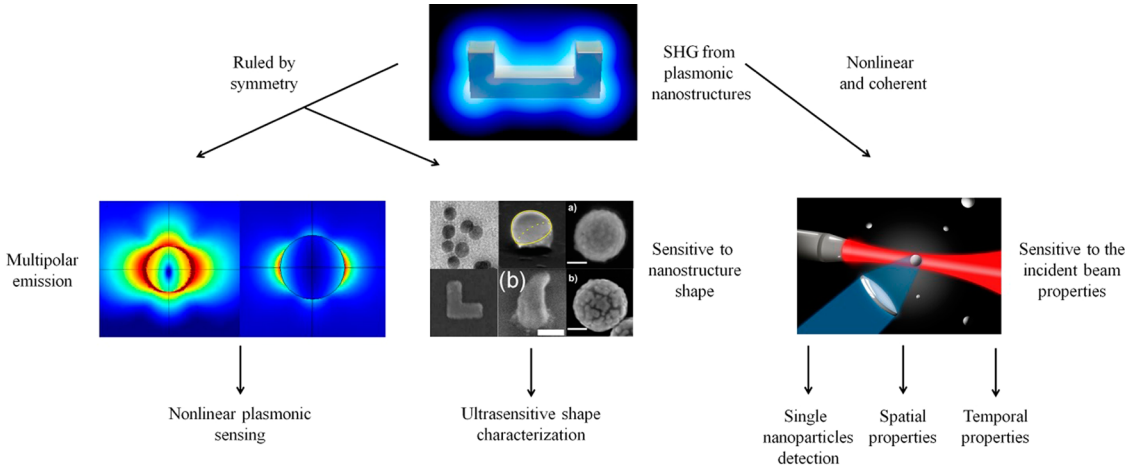

Figure 1. Outline of this review with the different links between fundamental principles of SHG in plasmonic nanostructures and practical applications. Reprinted from ref 9. Copyright 2010 American Chemical Society. Reprinted with permission from ref 10. Copyright 2010 American Physical Society. Reprinted from ref 11. Copyright 2011 American Chemical Society. Reprinted from refs 12, 147, and 182. Copyright 2012 American Chemical Society. Reprinted from ref 150. Copyright 2014 American Chemical Society.

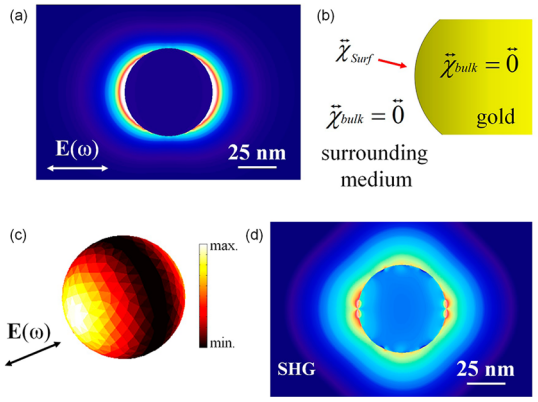

Figure 2. SHG from a 50 nm spherical gold nanoparticle in water. (a) Fundamental near-field intensity induced by an incident planewave (λ = 800 nm). (b) Schematics explaining the surface origin of SHG. (c) Spatial distribution of the nonlinear polarization over the nanoparticle surface. (d) SH near-field intensity shown in a log scale. All the computations have been performed with a surface integral equation (SIE) method.

and chemists looking for new optical sensing techniques.

Origin of SHG in Plasmonic Nanostructures. SHG is a nonlinear optical process of the second order,[3,4] whereby two photons at the fundamental frequency ω (corresponding to the frequency of the incident light) are converted into one photon at the second harmonic (SH) frequency $\Omega = 2\omega$.[23] Within a classical electromagnetic description, the source to the SHG light is the nonlinear polarization $\mathbf{P}(\Omega)$ oscillating at the SH frequency.[3,4] In the electric dipole approximation, the nonlinear polarization results from the interaction of the fundamental electric field $\mathbf{E}(\omega)$ with the nonlinear medium, the properties of which are given by the second-order nonlinear susceptibility tensor $\chi^{(2)}$ (see Figure 2):

$$\mathbf{P}(\Omega) = \chi^{(2)} : \mathbf{E}(\omega)\mathbf{E}(\omega) \tag{1}$$

The second-order nonlinear susceptibility $\chi^{(2)}$ is a third-rank tensor, and its elements describe the electronic and the symmetry properties of the considered nonlinear material. Plasmonic nanostructures are made of lossy materials, and these elements are, in general, complex valued. The first step to describe SHG is to determine the properties of the second-order nonlinear susceptibility. It is well-established that SHG is forbidden in centrosymmetric media in the electric dipole approximation.[24−27] Indeed, if the sign of the applied field is changed, the sign of the polarization must also change:

$$\begin{aligned} -\mathbf{P}(\Omega) &= \chi^{(2)} : (-\mathbf{E}(\omega))(-\mathbf{E}(\omega)) \\ &= \chi^{(2)} : \mathbf{E}(\omega)\mathbf{E}(\omega) \end{aligned} \tag{2}$$

Comparison with eq 1 leads to $\mathbf{P}(\Omega) = -\mathbf{P}(\Omega)$, which can only occur if $\mathbf{P}(\Omega) = 0$, demonstrating that the nonlinear susceptibility $\chi^{(2)}$ must vanish in centrosymmetric media. In the main plasmonic metals (gold, silver, copper, or aluminum), the atoms are organized in a face-centered cubic lattice, which is a centrosymmetric unit pattern, and SHG is thus forbidden in the bulk of these metals in the electric dipole approximation. As a consequence, a lack of centrosymmetry is required for allowing the emission of SH light. This necessary symmetry breaking can be induced either by the medium or by the electromagnetic field properties. In the first case, the centrosymmetry is locally broken at the metal surface because of the finite dimension of the atomic lattice. This property gives rise to surface SHG (see Figure 2b).[24−27] When the surface anisotropy is neglected, only the $\chi^{(2)}_{\perp\perp\perp}$, $\chi^{(2)}_{\perp\parallel\parallel}$, and $\chi^{(2)}_{\parallel\parallel\perp} = \chi^{(2)}_{\parallel\perp\parallel}$ components of the nonlinear susceptibility $\chi^{(2)}$ do not vanish. Here, $\perp$ denotes the normal component perpendicular to the interface and $\parallel$ denotes the tangential component. For plasmonic metals, the $\chi^{(2)}_{\perp\perp\perp}$ component of the nonlinear susceptibility is the largest component of the surface nonlinear susceptibility by at least 1 order of magnitude.[28−30] The amplitude of the $\chi^{(2)}_{\perp\perp\perp}$ component of the nonlinear surface susceptibility has been measured for different flat metallic films at a pump wavelength of 800 nm, leading to the following values: 2.3×10^{-13} cm^2/statvolt for gold, 3.2×10^{-13} cm^2/statvolt for silver, 1.5×10^{-13} cm^2/statvolt for copper, and 30×10^{-13} cm^2/statvolt for aluminum.[30] The nonlinear surface susceptibility of aluminum is 1 order of magnitude higher than that of other metals, explaining the recent interest in nonlinear plasmonics based on aluminum.[13,31,32] Beyond the electric dipole approximation, the spatial variation of the electromagnetic field can also break the centrosymmetry, and nonlocal bulk terms are theoretically possible.[33] Although plasmonic materials are not always crystalline, one can write for cubic materials:

$$\begin{aligned} \mathbf{P}_{bulk}(\mathbf{r}, \Omega) = {} & \beta_{bulk}\mathbf{E}(\omega, \mathbf{r})[\nabla \cdot \mathbf{E}(\omega, \mathbf{r})] \\ & + \gamma_{bulk}\nabla \cdot [\mathbf{E}(\mathbf{r}, \omega) \cdot \mathbf{E}(\mathbf{r}, \omega)] \\ & + \delta'_{bulk}[\mathbf{E}(\omega, \mathbf{r}) \cdot \nabla]\mathbf{E}(\omega, \mathbf{r}) \end{aligned} \tag{3}$$

where β_{bulk}, γ_{bulk}, and δ'_{bulk} are physical parameters related to the metal properties describing the electric quadrupole and magnetic dipole interactions. Here, the term "nonlocal" refers to the field gradient involved in these contributions (the nonlinear polarization at one point depends on the fundamental electric field at other points) as opposed to the dipolar local surface contribution for which the nonlinear polarization at one given point of the surface depends on the fundamental electric field at this point only. Contrary to the surface contribution, which spreads over a few atomic layers only (*i.e.*, several angstroms), the bulk contribution extension is limited by the finite penetration depth of the electromagnetic field in the metal (*i.e.*, tens of nanometers). Bulk contributions are naturally included in the hydrodynamic model and free-electron theories

of metals[24,33−39] but have also been included in surface formalisms.[40,41] However, the experimental separation of bulk and surface contributions is not an easy task due to the presence of "bulk-like" surface contributions induced by the fast field variation at the metal interface.[42,43] This challenge has been recently tackled using the two-beam SHG configuration for a flat gold film[28] and the fitting of SHG from gold nanospheres with full wave computations,[29] demonstrating that the bulk contributions are weaker than the surface terms and the $\chi^{(2)}_{\perp\perp\perp}$ component, in particular.[28,29] Although the $\chi^{(2)}_{\perp\perp\perp}$ component of the surface susceptibility is sufficient to describe most of the experimental results, both surface and bulk effects should be ideally taken into account for an accurate description of the systems at hand since both could be observed, depending on the experimental conditions.[28,29]

Another important fundamental question relates to the electronic origin of SHG. The hydrodynamic model considers that the nonlinearity arises from the motion of the conduction electrons only,[24,33−39] although electronic transitions from the d-band to the conduction sp-band may also contribute significantly to the nonlinear susceptibility, a consequence of the high density of states in the d-band.[44] Furthermore, the time-dependent density functional approach has revealed that electronic surface states enhance the nonlinearity.[45,46] The influence of nonlinear quantum tunneling on the SH conversion yield from strongly coupled nanoparticles has also been recently investigated.[47,48] Although the exact electronic origin of SHG in metals is still under investigation, the surface contribution is involved in all of the derived theoretical models and indubitably plays an important role in SHG.

Multipolar SH Emission. The difference between the linear and SH responses of metallic nanoparticles is explained by the centrosymmetry sensitivity of SHG. The sources of SHG are distributed over the nanoparticle surface (see Figure 2), and if the nanoparticle shape is centrosymmetric, the SH intensity vanishes in the far-field in the electric dipole approximation; that is, the SH wavelets generated by the SH sources distributed over the nanoparticle surface perfectly cancel each other out in the far-field. Therefore, additional physical mechanisms are required for the observation of SHG, and the centrosymmetry must be broken a second time but at a larger scale. As discussed previously in the case of the microscopic origin of SHG, this second symmetry breaking must be induced either by the geometry, by the nanoparticle shape, or by the field variation over the plasmonic source and requires a physical description beyond the electric dipole approximation. Since SHG is a nonlinear process involving two electromagnetic waves, the fundamental incident wave and the wave scattered at the SH frequency, retardation effects can arise both at the excitation and

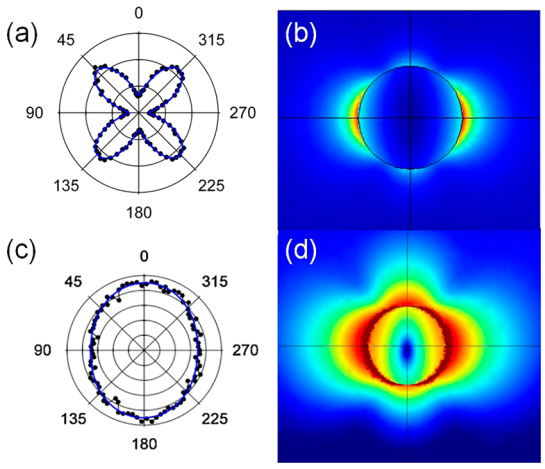

Figure 3. Multipolar emission from perfect nanospheres. (a) Experimental evidence of the SH quadrupolar emission from 150 nm gold nanoparticles and (b) corresponding near-field intensity. (c) Experimental evidence of the interference between dipolar and octupolar emission in the SHG from 100 nm gold nanoparticles and (d) corresponding near-field intensity. Panels (a,b) reprinted from ref 9. Copyright 2010 American Chemical Society. Panels (c,d) reprinted with permission from ref 10. Copyright 2010 American Physical Society.

emission stages. SHG can therefore be understood by considering the different modes (dipole, quadrupole, and so on) involved in the process. At the first order of retardation, the most efficient mechanism for a dipolar SH emission is the $E_1 + E_2 \rightarrow E_1$ channel. Here, the standard formalism is used: the two terms on the left of the arrow refer to the nature of the two exciting fundamental modes, whereas the right term describes the SH emission mode. Explicitly, this $E_1 + E_2 \rightarrow E_1$ mechanism corresponds to a dipolar SH emission E_1 arising from the combination of an electric dipole mode E_1 and an electric quadrupole mode E_2. This SH dipolar emission requires therefore retardation at the excitation stage. In this framework, the $E_1 + E_1 \rightarrow E_1$ channel, which can be the dominant contribution in noncentrosymmetric nanostructures, is forbidden in centrosymmetric nanostructures since the parity is not conserved. Retardation effects are obtained with the introduction of the quadrupolar mode E_2 in the description of the interaction between the nanoparticle and the incident field at first order. On the other hand, the quadrupolar SH emission can be excited without any retardation in the field at the fundamental frequency (Figure 3a,b). This latter mode corresponds to the $E_1 + E_1 \rightarrow E_2$ channel and corresponds to a quadrupolar SH emission E_2 arising from the interaction of an electric dipole mode E_1 with itself. Neglecting all resonance enhancements, the dipolar and quadrupolar emission modes have the same dependence with the scattering parameter $x = ka$, where a is the nanostructure size, that is, for a nanosphere, its diameter, and k is the fundamental wavevector. Both retarded E_1 and E_2 modes scattered at the SH

frequency scale with an x^6 dependence contrary to the nonlinear nonretarded E_1 mode scaling with x^4 as a purely surface response and the linear Rayleigh scattering mode scaling with k^4a^6. This difference is a direct consequence of the requirement of retardation effects in SHG from centrosymmetric nanostructures. However, the relative weight of these multipoles in SHG can be modified by the proximity of surface plasmon resonances. Dipole and quadrupole surface plasmon resonances indeed have a different energy. The multipolar nature of the SHG from spherical metallic nanoparticles with various sizes and made of different materials has been widely discussed in the literature.[49−54] In particular, it has been experimentally demonstrated, using hyper-Rayleigh scattering, that even and odd SH modes are perfectly decoupled when the SH intensity is collected perpendicularly to the direction of the incident fundamental laser beam. In this specific experimental configuration, even and odd SH emission modes are selected using an analyzer since they are polarized perpendicular and parallel to the scattering plane, respectively. Interference between multipoles has nevertheless been observed too for SHG (Figure 3c,d).[10] This multipolar nature is an important feature of the SHG response from metallic nanostructures and has been investigated for nanoparticles with varying shapes as nanorods, which are centrosymmetric despite a lower symmetry than that for spheres, for example.[55−59]

Shape Effects in Basic Geometries. Because of the centrosymmetry rule, the design of nanostructures with noncentrosymmetric shapes has become essential. Nowadays, both top-down and bottom-up approaches have been optimized for the fabrication of nanoparticles with excellent reproducibility. The SHG response from chemically synthesized and lithographed nanoparticles with various geometries has been investigated (Figure 4). Almost any shape can be designed, and such geometries include, for instance, gold nanostars,[60] silver triangular nanoprisms,[61] holes in metallic films,[62−66] curved nanorods,[67] split-ring resonators with U-shape,[68−70] metal−dielectric nanodisks,[71] gold T-dimers,[72] nanocups,[11] chiral G-shaped nanoparticles,[73−78] chiral helix,[79−81] L-shaped nanoparticles,[12,82−85] or gold nanotips.[86−88] These various nanoparticle shapes exacerbate specific features of the nonlinear response and were thus designed for different purposes. For example, L-shaped nanoparticles are basic plasmonic elements with noncentrosymmetric shapes and are efficient to increase the overall SHG intensity in the backward and forward directions. Split-ring resonators support magnetic modes sustaining also high SHG intensities, besides being the elementary constitutive elements for a huge variety of metamaterials. Chiral nanostructures have also been designed; the SHG response from these structures depends on the handedness of the incident light leading to the so-called SH circular dichroism.[77,89,90] Superchiral

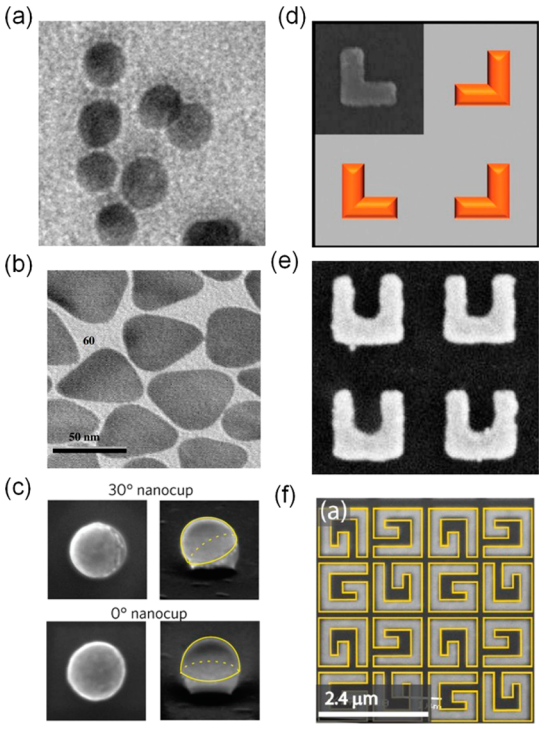

Figure 4. Examples of structures the SHG of which has been studied. Chemically synthesized nanoparticles: (a) 20 nm gold nanoparticles, (b) silver nanoprisms,[61] and (c) gold nanocups.[11] Lithographed nanoparticles: (d) L-shaped nanoparticles,[12] (e) gold split-rings,[70] and (f) chiral G-shaped nanoparticles.[73] Panels (a,b) reprinted with permission from ref 61. Copyright 2009 Elsevier. Panel (c) reprinted from ref 11. Copyright 2011 American Chemical Society. Panel (d) reprinted from ref 12. Copyright 2012 American Chemical Society. Panel (e) reprinted with permission from ref 70. Copyright 2012 American Physical Society. Panel (e) reprinted from ref 73. Copyright 2009 American Chemical Society.

metasurfaces combine the chirality of light with that of nanostructures and induce strong SH intensities.[91] Besides the study of nanostructures, that of nanoholes in metal nanofilms has also been performed as reciprocal systems in the sense of Babinet principle for nanostructures. The possibility to observe extraordinary light transmission, where the transmitted intensity is much higher than the one expected from the geometric aperture area, has driven this research.[92] In comparison with nanoparticles, nanoholes and nanocavities can support higher incident peak intensities due to the fast heat dissipation in the metallic film, resulting in a higher damage threshold.

It is interesting to note that a noncentrosymmetric shape does not necessarily result in a stronger SHG intensity, and further symmetry issues can arise despite the lack of centrosymmetry. For example, the nonlinear efficiency of noncentrosymmetric decahedra with fivefold symmetry is identical to that of centrosymmetric spheres with identical sizes due to the cancellation of the nonlinear emissions from their different facets.[93] A symmetry relation often encountered in this framework, and particularly in the case of nanoparticle

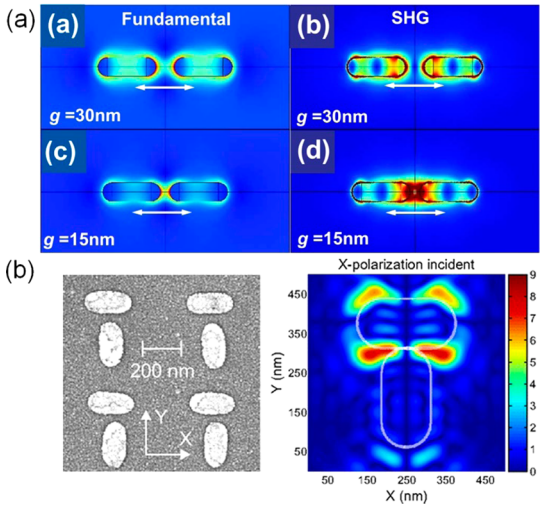

Figure 5. SHG from coupled nanoparticles: (a) gold nanoantennas and (b) gold T-dimers. Panel (a) reprinted with permission from ref 98. Copyright 2010 Optical Society of America. Panel (b) reprinted from ref 72. Copyright 2007 American Chemical Society.

arrays, is the mirror symmetry. If a mirror symmetry is actually present, then the SH wave propagating along the forward and backward directions is polarized in the symmetry plane due to the spatial reversal of the nonlinear polarization and cancels in the other direction.[77,94−96] A dramatic consequence arises when the nanoparticle array exhibits two orthogonal mirror planes: the SH intensity vanishes in these directions, although the constituting nanoparticles are not centrosymmetric.[12] This particularity must be kept in mind for the design of nanostructure arrays. It may also result in surprising observations for coupled nanostructures (Figure 5). One could naively think that the high fundamental field observed in narrow gaps[97] induces a strong SHG. Actually, this is not the case, and the reverse, the silencing of the SHG from plasmonic nanoantennas, has been pointed out.[98] Although the strong field enhancement observed in the gaps at the fundamental wavelength results indeed in a strong nonlinear polarization,[99] the nonlinear polarization vectors standing at each sides of the nanogap are out of phase and their contributions to the SH wave tend to cancel out in the far-field region.[98,99] This silencing of the SHG response is partially suppressed in nanogaps with noncentrosymmetric geometries, as those observed in gold nanoparticle dimers with T-shapes[72] or structures composed of two arms with different sizes.[100,101] This silencing is a direct consequence of the symmetry properties of SHG and, as such, is not detected for third-order nonlinear optical processes such as THG and FWM.[18,19] These examples further emphasize one more time the unique properties of SHG.

In this review, a clear separation has been made between the centrosymmetry breaking induced by the nanoparticle shapes and the electromagnetic fields.

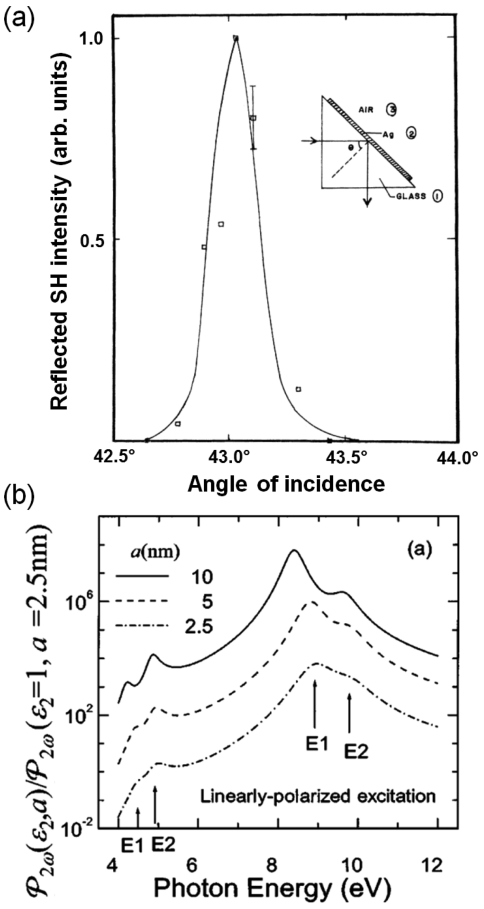

Figure 6. Plasmon enhancement of the SHG from (a) silver film[103] and (b) Al nanospheres with different sizes.[108] Panel (a) reprinted with permission from ref 103. Copyright 1974 American Physical Society. Panel (b) reprinted with permission from ref 108. and Copyright 1999 American Physical Society.

The distinction is, however, not unambiguously defined since both effects are deeply interconnected. The case of spherical nanoparticles is a good example to illustrate this remark. For the smallest nanoparticles, the origin of the SH response is their nonperfectly symmetric shape (Figure 4a), but as the nanoparticle size increases, the role played by the retardation effects becomes more important.[102] The transition from a dipolar SH emission induced by shape effects to a quadrupolar SH emission induced by retardation is a good example of the interconnection between the geometry of the nanostructure (size, shape, etc.) and the properties of the electromagnetic fields at both the fundamental and SH frequencies.[102]

Plasmon Enhancement and Advanced Nanostructures for Efficient SHG. Equation 1 clearly emphasizes that SHG increases nonlinearly with the fundamental electric field amplitude. The basic idea behind nonlinear plasmonics is to use the enhanced electric field associated with plasmon resonances to increase the strength of nonlinear optical effects (Figure 6).[8] The first plasmon enhancement of SHG was reported in 1974 for surface

plasmon polaritons propagating at the surface of a silver film (Figure 6a).[103] In one of the first experiments in nonlinear plasmonics, it was observed that the reflected SH intensity increases by several orders of magnitude when the incident angle permits surface plasmon polaritons to launch, demonstrating that they have the ability to increase the nonlinear signal.[103] The LSPR enhancement of SHG from metallic nanoparticles has also been theoretically predicted and experimentally confirmed.[104,105] Due to the LSPR enhancement, SHG from plasmonic nanostructures is much higher than that from the best chromophores[106] and comparable to that from nanoparticles made of nonlinear materials as potassium niobate ($KNbO_3$), lithium niobate ($LiNbO_3$), barium titanate ($BaTiO_3$), potassium titanyl phosphate ($KTiOPO_4$, KTP), and zinc oxide (ZnO).[107] In plasmonic structures with nanometer sizes, an enhancement of the SH intensity is clearly observed when the wavelength of the incident light matches the resonant wavelength of a LSPR (Figure 6b).[108,109] However, SH emission spectra are much more complex than the corresponding linear spectra since multiple resonances may be observed. Resonances can indeed occur at either the fundamental or the SH frequencies. This multiple resonance response has been observed, for instance, in the SH emission from aluminum spheres with the fundamental/SH photons matching the dipolar E_1 or quadrupolar E_2 wavelengths (see Figure 6b). For the manipulation of the SHG resonance enhancements, Fano resonances have appeared to be particularly efficient. Fano resonances arise from the coupling between optical dark and bright modes.[110−122] These particular resonances are characterized by their asymmetric line shapes that arise from the interaction between a narrow plasmonic dark mode and a broad plasmonic bright mode. This interaction results in the ability to tailor the fundamental near-field distribution over the different nanoparticles and then in the control of the driven nonlinear surface polarization.[123,124] The underlying control mechanism is then based on the mastering of the coupling strength.

To increase the SHG in nonlinear crystals, it is necessary to satisfy the phase-matching conditions in order to ensure an efficient energy transfer from the fundamental wave to the SH wave, by the use of birefringence, for example. However, this important paradigm of NLO is not anymore applicable to plasmonic nanostructures since their dimensions are much smaller than the wavelength. It is therefore necessary to find other means for a high nonlinear conversion at the nanoscale. Indeed, SHG from plasmonic nanostructures must be considered as a nonlinear scattering phenomenon and not as a phase-matched process. In this context, the design of multiresonant nanostructures has been proved to be a very efficient approach, substituting phase matching with mode matching (see Figure 7). Indeed, the fundamental wavelength (for example λ = 800 nm) is twice the SH wavelength (λ = 400 nm in this case), and both waves are well separated spectrally. The electromagnetic properties of a plasmonic system can be specifically optimized at these two wavelengths in order to reach an efficient excitation at the fundamental wavelength and a maximal emission at the SH wavelength. Figure 7a shows an example of such a multiresonant nanostructure optimized for SHG at 400 nm, the so-called double resonant antenna (DRA).[31] The DRA was made of aluminum, instead of gold, in order to prevent LSPR damping induced by the interband transitions at the SH frequency[125] and to exploit the high nonlinear surface susceptibility of aluminum.[30] Numerical simulations have revealed the resonant behavior of the DRA at both 400 and 800 nm, and experimental results confirmed that the SH intensity from the DRA is higher than that from a simple nanoantenna with only one resonance at the fundamental wavelength (800 nm).[31] Other designs, such as multiresonant log-periodic optical antennas[126] and mode-matched V-shaped nanoantennas,[127] have been also proposed in order to increase the SHG efficiency. However, these nanostructures operate in the near-infrared since they are fabricated in gold. Indeed, the high losses associated with the interband transitions in gold for a wavelength shorter than ~500 nm do not permit well-defined LSPR to be observed in this spectral range. The design of multiresonant structures has also been combined with Fano resonances at the fundamental wavelength.[110,111] Indeed, an optical dark mode can be efficiently excited at the Fano resonance through its coupling with an optical bright mode.[110,111] A stronger near-field enhancement is associated with such a dark mode, due to its ability to store the electromagnetic energy at the nanoscale.[120] Consequently, SHG benefits from the presence of a Fano resonance at the fundamental wavelength.[128−130] Another approach used for the optimization of SHG from nanoparticle arrays is to combine active elements (nanoparticles with noncentrosymmetric shapes) and passive elements (nanoparticles with centrosymmetric shapes).[131] The LSPRs of the active and passive particles are at distinct wavelengths, but the passive particles modify the electromagnetic modes of the total array and enhance the SHG from the active nanoparticles.[131] Furthermore, the yield of SHG from a nanoparticle array depends not only on the nanoparticles' geometry but also on their spatial organization.[12] Hybrid nanostructures, composed of a plasmonic part for the enhancement of the electric field and another material with a noncentrosymmetric atomic lattice for efficient SHG, were proposed for an even stronger nonlinear conversion at the nanoscale.[132,133] In a clever design, tetragonal $BaTiO_3$ nanoparticles were covered with gold nanoshells, resulting in a SH intensity much higher (~100 times) than that of a simple (nonresonant) gold

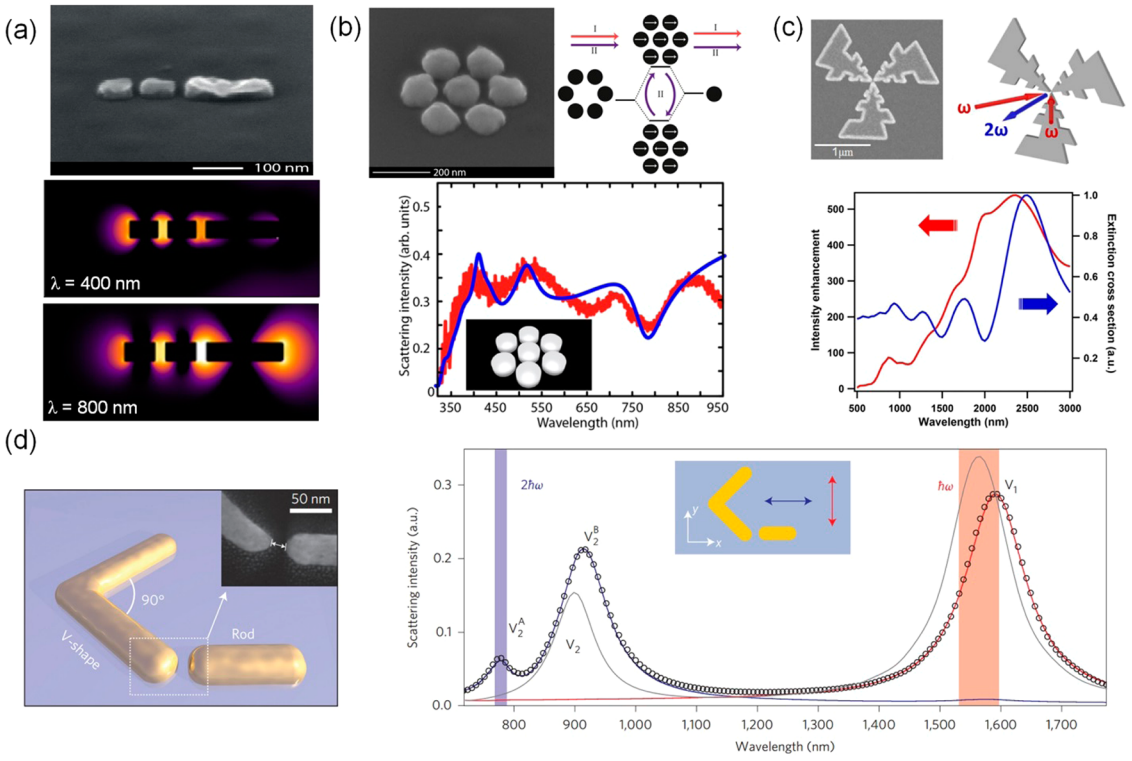

Figure 7. Examples of multiresonant nanoantennas optimized for SHG: (a) aluminum double resonant antenna composed of three arms, (b) silver heptamer supporting a Fano resonance at the fundamental wavelength, (c) multiresonant log-periodic optical antennas, and (d) mode-matched V-shaped nanoantenna. Panel (a) reprinted with permission from ref 31. Copyright 2012 Optical Society of America. Panel (b) reprinted from ref 129. Copyright 2013 American Chemical Society. Panel (c) reprinted from ref 126. Copyright 2012 American Chemical Society. Panel (d) reprinted with permission from ref 127. Copyright 2015 Nature Publishing Group.

sphere and much higher (~500 times) than that of a bare $BaTiO_3$ nanoparticle.[134]

Single Nanoparticle Detection. As emphasized in the previous section, SHG is very sensitive to the nanoparticle shape. Despite recent advances in nanofabrication, it is still impossible to produce extended nanoparticle assemblies with the exact perfect same design, and small shape deviations are always observed, irrespective of the fabrication technique. For this reason, the response of a single nanoparticle can dramatically differ from the behavior of an ensemble or array of isolated (*i.e.*, noninteracting) nanoparticles. Therefore, single nanoparticle measurements are mandatory for a full understanding of the nonlinear response. In the linear regime, single nanoparticle experiments have been performed with different methods like dark-field measurements as well as spatial modulation spectroscopy,[135] in order to remove the strong incident light.[136,137] In SHG experiments, the challenge is quite different. In this case, the incident light is easily removed with optical filters since SHG occurs at half the wavelength of the incident light. However, the SH signal is much weaker, down to few hundreds to just a few photons/s, than the signals observed for other nonlinear optical processes like two-photon photoluminescence, for example. Long acquisition times, up to hours, are required even though femtosecond lasers are used to increase the nonlinear conversion. These laser sources provide a high peak power with a weak energy per pulse, allowing for long experimental acquisition times without inducing sample damages. The first observation of SHG from single metallic nanoparticles was reported in 2004.[138] Jin *et al.* deposited silver nanoparticles on a Si_3N_4 thin film and performed a scan of the sample recording the SH intensity as a function of the sample position. Markers were used for both the optical measurements and the electronic microscopy in order to correlate the morphology of the nanoparticles with their nonlinear signal. This experiment demonstrated, in particular, that the silver nanorods are efficient only when the incident wave is polarized along their long axis (Figure 8a).[138] However, the interaction between a single nanoparticle and the substrate breaks the centrosymmetry, and the intrinsic SH response of a single nanoparticle cannot be directly measured since this symmetry breaking competes with that induced by the nanoparticle shape. To alleviate this problem, one can embed the nanoparticle in a homogeneous medium, either gelatin or a polymer, PAA, for example, in order to re-establish the centrosymmetry in the vicinity of the nanoparticle (Figure 8b).[9,139] When the nanoparticle concentration is low enough and a sensitive detection scheme is used,[140] maps of the SH intensity reveal the positions of single nanoparticles in

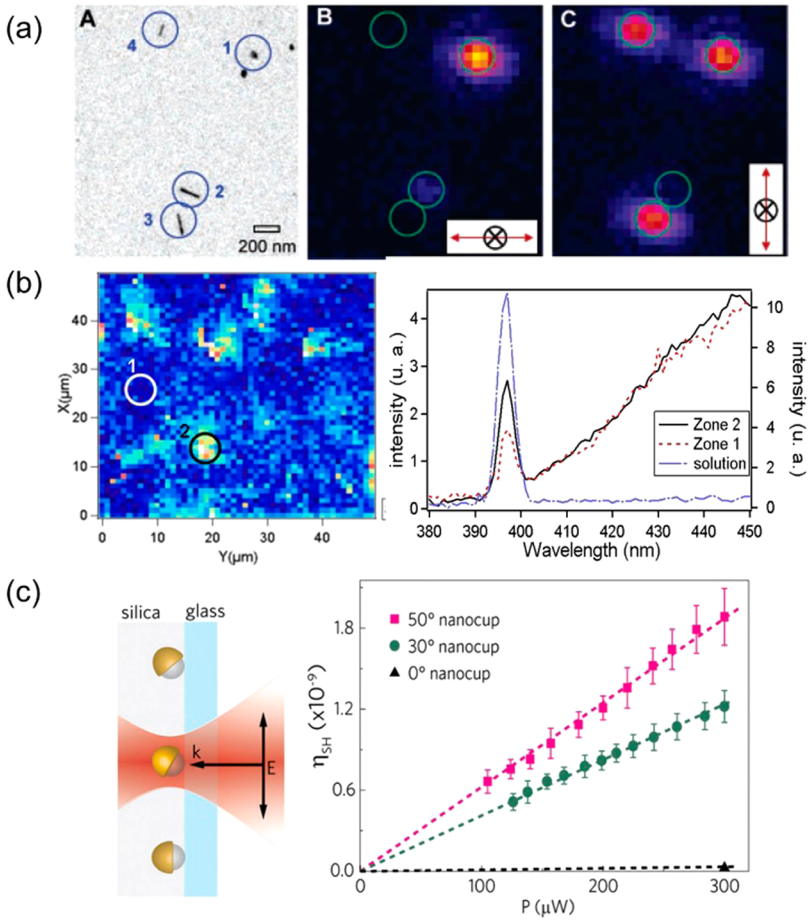

Figure 8. Detection of the SHG from single metallic nanoparticles. (a) Silver nanospheres and nanorods deposited on a flat substrate. Reprinted from ref 138. Copyright 2005 American Chemical Society. (b) Single gold nanoparticles embedded in a homogeneous gelatin matrix. Reprinted from ref 9. Copyright 2010 American Chemical Society. (c) Single gold nanocups embedded in a silica layer. Reprinted from ref 11. Copyright 2011 American Chemical Society.

the transparent matrix. Recording consecutive 2D maps for several positions of the sample along the laser beam gives access to their 3D spatial distribution.[139] Similarly to two-photon microscopy, this technique exploits the intrinsic nonlinearity of SHG, which results in a narrower spread function of a laser beam since the spatial distribution of $I^2(\omega)$ is obviously narrower than that of $I(\omega)$. These experiments have been performed with 150 nm spherical gold nanoparticles.[9,139] Since nanospheres are invariant by rotation, there is no need for the measurement of their orientation. This is no longer the case for noncentrosymmetric nanoparticles (see Figure 8c). The SHG from single nanocups embedded in a thin silica matrix has been recorded as a function of the incident power and the nonlinear efficiency correlated to the nanocup orientation.[11] Although the SHG vanishes for nanocups oriented normally to the incident beam, a tilt of the cup is easily observed thanks to a magnetic dipolar mode arising at the fundamental wavelength.[11] In these experiments, the SH intensity has been recorded in the far-field region. The SHG from single gold nanoparticles has also been investigated in the near-field region using an optical fiber for the excitation and compared to the atomic force microscope topology.[141]

Nonlinear Characterization of Structural Properties. We now turn our attention to the practical applications of SHG in plasmonic nanostructures and consider first the nonlinear optical characterization of structural properties. Indeed, as a consequence of the influence of centrosymmetry, SHG varies considerably with the nanostructure shape, opening the way to *in situ* ultrasensitive nonlinear optical characterization techniques. Indeed, SHG is able to reveal any small deviation from perfectly symmetric shapes[102,142] and small surface roughness.[143−145] This is very appealing since SHG can reveal defects that do not modify the linear response at all but are encoded in the SH emission pattern (see Figure 9a).[145−147] For some specific nanoparticle geometries, beam shaping and polarization state definition are necessary for a good coupling between the incident laser field and LSPR, as demonstrated in the case of the nonlinear optical characterization of gold nanotips with cylindrical vector incident beams with azimuthal and radial polarizations (see Figure 9b).[147] What is even more interesting is that

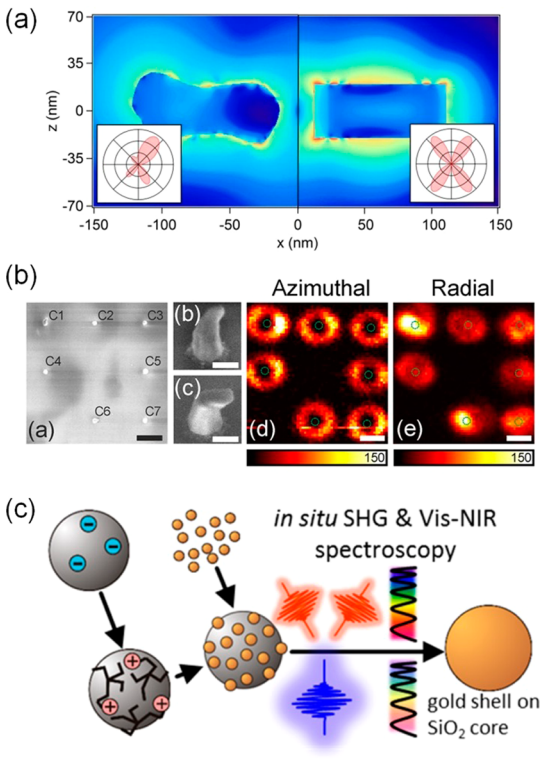

Figure 9. Nonlinear optical characterization of plasmonic nanoparticles using SHG. (a) Numerical study comparing the SHG from a realistic nanoantenna with that from an idealized one. Reprinted from ref 145. Copyright 2013 American Chemical Society. (b) Imaging of gold nanotips using cylindrical vector incident beams. Reprinted from ref 147. Copyright 2012 American Chemical Society. (c) *In situ* monitoring of gold nanoshell growth using SHG. Reprinted from ref 150. Copyright 2014 American Chemical Society.

SHG can provide useful information on the chemical synthesis of plasmonic nanoparticles, beyond the characterization of finalized samples. Indeed, the *in situ* monitoring of the different synthesis steps is important for a good control of the final nanoparticle shapes and size dispersions.[148,149] For example, the growth of gold shells on silica cores has been simultaneously monitored with UV−visible spectroscopy and HRS during the chemical synthesis of gold nanoshells (see Figure 9c).[148] These experiments have shown that the SH intensity rises to a maximum before the complete closure of the gold shells. This was attributed to the surface roughness and the nonsymmetric hot spot distribution over the nanoparticle surface.[150] This approach has been also used for monitoring the chemical synthesis of gold nanostars[60] and gold nanoparticles aggregation,[151] demonstrating its range of applications.

Another challenge in nanophotonics is the evaluation of distances as small as a few nanometers using optical waves. This demanding task can be performed by using the interaction between plasmon modes since the coupling strength changes significantly with the distance, allowing the design of plasmon nanorulers, the optical responses of which vary with the conformation of the different nanoparticles that compose them.[152−157] In order to observe biological and chemical processes with the best spatial resolution, it is important to design compact plasmon nanorulers.[152−157] Following an approach proposed in the linear regime by Liu *et al.*,[158] a nonlinear plasmon nanoruler, composed of only three nanorods instead of five for its linear counterpart, has been recently designed.[123] Taking advantage of the symmetry properties of SHG, the conformation and the nanorod position can be unambiguously determined.[123]

Laser Beam Characterization. The introduction of this review emphasizes that NLO is deeply connected with research in the physics of lasers. SHG from plasmonic nanostructures may therefore be used in laser beam characterization. We already mentioned that it is possible to tailor the incident laser beam properties in order to guarantee a strong coupling between the investigated nanostructures and the incident electromagnetic field, but the inverse is also true: it is possible to use SHG from single nanostructures to probe the properties of highly focused laser beams much below the diffraction limit with a high accuracy. Let us first consider the determination of the spatial features of the laser beam. Figure 10a shows how the longitudinal component of a strongly converging Gaussian (HG00) beam can be probed with the SHG from a single gold nanotip.[159] The tip is moved in the laser spot, and the map of the SH intensity reveals two positions for which the coupling between the gold nanotip and the incident laser beam is excellent. These positions correspond to the ones with a strong longitudinal component of the incident electric field, emphasizing that the vector nature of the incident electric field can be probed at the nanoscale using SHG.[159]

On the other hand, the observation of SHG from plasmonic nanoparticles requires the use of ultrashort (femtosecond) laser systems. To satisfy the conjugated observable principle, ultrashort femtosecond pulses (∼30 fs and shorter) have a very large bandwidth (up to several hundreds of nanometers). Due to the dispersive optical elements used in experimental setups, the different spectral components of femtosecond pulses do not reach the sample at the same time, and the SHG is not very efficient (see the green curves in Figure 10b).[160,161] Accanto *et al.* have proposed to use a preconditioning scheme, before the experimental setup, in order to compensate the unfavorable effects of dispersion in nonlinear plasmonic experiments.[160,161] After several optimization rounds, the SH intensity is increased by several orders of magnitude (see the black curves in Figure 10b), demonstrating that the SHG from plasmonic nanoparticles can be used to check the temporal features of femtosecond laser pulses with a spatial resolution of ∼100 nm.[160,161]

Nonlinear Plasmonic Sensing. Applications benefiting from the fundamentals and basic ideas exposed above can then be envisaged, like nonlinear plasmonic

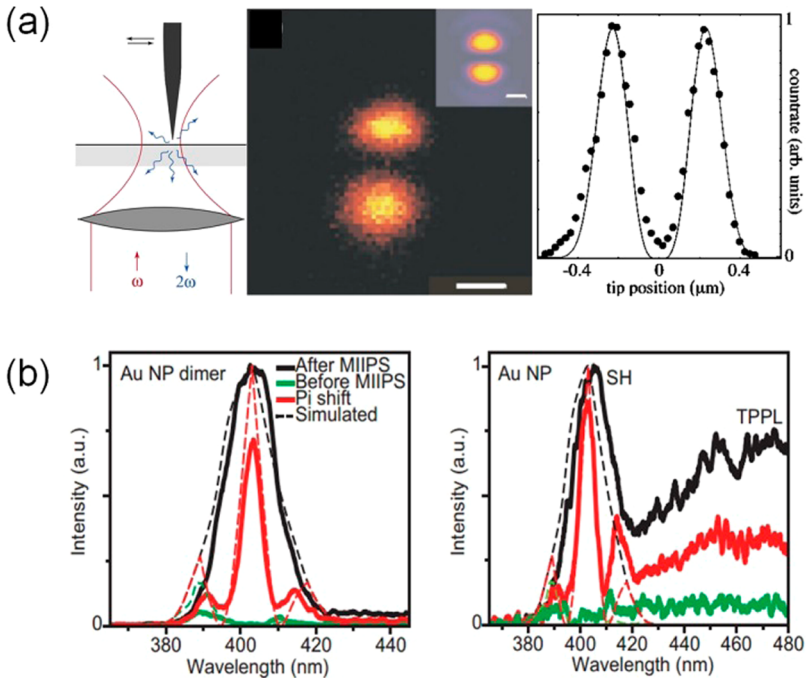

Figure 10. Optical beam characterization. (a) Longitudinal component of a strongly converging Gaussian (HG00) beam probed with the SHG from a gold nanotip. Reprinted with permission from ref 159. Copyright 2003 American Physical Society. (b) Optimization of the compression of femtosecond laser pulses using the SHG from single gold nanoparticles. Reprinted with permission from ref 160. Copyright 2014 Nature Publishing Group.

sensing. Before discussing how the SHG multipolar nature can be used in sensing, it is worth saying few words about the current developments in nonlinear plasmonic sensors. Indeed, one of the most promising applications in plasmonics is the sensing of chemical and biological entities, making use of the SPR-enhanced sensitivity.[162−169] Quickly, in the past, it has been realized that SHG from plasmonic nanostructures can be used to monitor chemical processes and to detect biological and chemical toxins with excellent sensitivity and selectivity.[170] SHG and HRS from gold nanoparticles were used to detect "spectroscopically silent" heavy metal ions (Pb^{2+}),[171] diagnose single-base-mismatch DNA hybridization,[172] selectively detect and identify *Escherichia coli* bacteria with gold nanorods,[173] detect Alzheimer's disease biomarkers,[174] or detect breast cancer cells using the SHG from oval-shaped nanoparticles.[175] All these examples demonstrate the extensive versatility of the method for applications. They are based on the same simple scheme. The gold nanoparticles are first functionalized, that is, capped with specific molecules or biomolecules. The capping agent is selected for its high affinity with the targeted chemical/biological species in order to make chemical bonds between the nanoparticles. Since the SH signal from small nanoparticle aggregates strongly differs from the nonlinear signal from a collection of noninteracting nanoparticles, the presence of the target species induces a dramatic increase of the SH intensity. In his review on the second-order nonlinear optical properties of nanomaterials, Ray provides the reader with a very informative table, where he compares the detection limit of this approach with the detection limit of other assays based on nanostructures.[170] This comparative study reveals that SHG is very efficient for the detection of *Escherichia coli* bacteria or the tau protein but is less efficient than surface-enhanced Raman scattering[176] and real-time polymer chain reaction[177] for the detection of DNA/RNA. It is also less efficient than nanoparticle-based surface energy transfer[178] and electrochemical approaches for the detection of mercury.[179] These tests clearly show that SHG is a method of choice for plasmonic sensing and is appealing for the development of new strategies.

Nevertheless, in order to increase further the sensitivity and the detection limit of nonlinear plasmonic sensors, several methods based on the specificity of the SHG response have been proposed. The comparison between different plasmonic sensors is not straightforward, though, and a universal performance indicator is required. For this reason, a figure of merit (FOM) has been introduced as the ratio between the sensitivity, expressing the spectral shift of the LSPR induced by a given variation of the refractive index of the surrounding medium, and the surface plasmon resonance full width at half-maximum (fwhm).[166,180] A LSPR shift is indeed more difficult to observe on a broad resonance. The width of the LSPR is related to the total losses of the plasmonic system and can be decomposed into intrinsic (ohmic) and scattering losses.[181] Thus, it is of importance to decrease the total

losses in order to reduce the LSPR width and to increase the FOM for the optimization of plasmonic sensors. One possibility, among others, is to design plasmonic sensors based on high-order LSPR, such as quadrupolar modes, in order to reduce the scattering losses and therefore the resonance fwhm.[182] However, these modes are weakly radiative and thus difficult to observe in the linear regime due to the presence of strong dipolar modes in the same spectral range. As discussed previously, quadrupolar modes E_2 naturally appear in the SHG response from centrosymmetric nanoparticles since a description beyond the electric dipole approximation is mandatory.[108,109,183−189] As a result, SHG is a well-suited optical tool to monitor the evolution of the quadrupolar LSPR, in particular, its shift.[182] The case of 60 nm silver nanoparticles is a good illustration of the benefit provided by this approach since the quadrupolar LSPR has a FOM = 9.5, while the dipolar LSPR has a FOM = 3.8 only. A FOM twice as large can be obtained by switching from the linear to the nonlinear response.[182] More complex nonlinear plasmonic sensors, combining the SHG properties with that of Fano resonances, have also been designed. Interestingly, the coupling between the dark and bright modes at a given fundamental wavelength varies with the refractive index of the surrounding medium. As a consequence, the distribution of the nonlinear polarization over the nanostructure surface changes with the changes of the refractive index of the surrounding medium. The SH far-field emission pattern is then modified accordingly.[124] Fano resonance enhancement of the SHG response in plasmonic nanostructures permits the design of very sensitive plasmonic sensors because a small variation of the refractive index of the surrounding medium leads to a strong asymmetry in the SH response. This strategy is promising to push further the detection limit of plasmonic sensors.[124]

CONCLUSIONS AND OUTLOOK

In this review, the basic principles of SHG have been summarized, emphasizing the role played by symmetry in both the origin of the nonlinearity (local surface *versus* nonloncal bulk contributions) and the shape dependence of the scattered SH wave. The relationship between the specific properties of SHG from plasmonic nanostructures and some advanced applications has been outlined. Despite the significant amount of theoretical and experimental works devoted to the SHG from plasmonic nanostructures, the electronic origin (the relative contributions of the conduction and core electrons) has not yet been unambiguously determined. We believe that it will be possible to reach such a description in the near future by the combination of the latest electronic structure methods with nonlinear theory.[190] This point is particularly important for the development of sensing applications based on SHG that combine surface sensitivity and electronic dependence.[191] This is rather appealing in the context of recent applications based on hot electrons in chemistry and photovoltaics, for example.[192−194]

In parallel to nanophotonics, the recent developments in electromagnetic metamaterials and metasurfaces have proposed new directions for applications and for the design of new optical elements.[195−197] In that context, concepts developed in the linear regime are currently extended to NLO and, more specifically, SHG.[198−201] In those artificial materials, the metallic parts are simultaneously responsible for the nonlinearity and for the control of the nonlinear radiation. The unique properties of such metamaterials break some important paradigms of NLO, such as the requirement of phase-matching conditions for an efficient nonlinear conversion of incoming light. For example, Suchowski *et al.* have shown that the phase-matching condition is automatically satisfied in an optical zero-index metamaterial, opening a new way for the design of nonlinear optical components.[202]

This review has focused on nanostructures made of the most common plasmonic metals (gold, silver, copper, and aluminum), but new materials supporting LSPR have recently emerged. Among those, graphene is probably one of the most promising thanks to its strong coupling to electromagnetic radiation and unique electronic properties.[203,204] Very few works discuss SHG from graphene, and our understanding of the underlying physical phenomena does not yet reach that of SHG in common plasmonics systems.[205−208] In the future, the unique properties of graphene will probably open up new possibilities and applications in nonlinear plasmonics, beyond those reported in this review.

Conflict of Interest: The authors declare no competing financial interest.

Acknowledgment. Funding from the Swiss National Science Foundation (project 200020_153662) and the Région Rhône-Alpes ARC6 program is gratefully acknowledged.

REFERENCES AND NOTES

1. Maiman, T. H. Stimulated Optical Radiation in Ruby. *Nature* **1960**, *187*, 493–494.
2. Franken, P. A.; Hill, A. E.; Peters, C. W.; Weinreich, G. Generation of Optical Harmonics. *Phys. Rev. Lett.* **1961**, *7*, 118–119.
3. Boyd, R. W. *Nonlinear Optics*; Academic Press: New York, 1992.
4. Shen, Y. R. *The Principles of Nonlinear Optics*; Wiley Classics Library: Hoboken, NJ, 2003.
5. Maier, S. A. *Plasmonics: Fundamentals and Applications*; Springer: New York, 2007.
6. Gramotnev, D. K.; Bozhevolnyi, S. I. Plasmonic Beyond the Diffraction Limit. *Nat. Photonics* **2010**, *4*, 83–91.
7. Schuller, J. A.; Barnard, E. S.; Cai, W.; Jun, Y. C.; White, J. S.; Brongersma, M. L. Plasmonics for Extreme Light Concentration and Manipulation. *Nat. Mater.* **2010**, *9*, 193–204.
8. Kauranen, M.; Zayats, A. V. Nonlinear Plasmonics. *Nat. Photonics* **2012**, *6*, 737–748.

9. Butet, J.; Duboisset, J.; Bachelier, G.; Russier-Antoine, I.; Benichou, E.; Jonin, C.; Brevet, P.-F. Optical Second Harmonic Generation of Single Metallic Nanoparticles Embedded in a Homogeneous Medium,. *Nano Lett.* **2010**, *10*, 1717–1721.
10. Butet, J.; Bachelier, G.; Russier-Antoine, I.; Jonin, C.; Benichou, E.; Brevet, P.-F. Interference between Selected Dipoles and Octupoles in the Optical Second-Harmonic Generation from Spherical Gold Nanoparticles. *Phys. Rev. Lett.* **2010**, *105*, 077401.
11. Zhang, Y.; Grady, N. K.; Ayala-Orozco, C.; Halas, N. J. Three-Dimensional Nanostructures as Highly Efficient Generators of Second Harmonic Light. *Nano Lett.* **2011**, *11*, 5519–5523.
12. Husu, H.; Siikanen, R.; Mäkitalo, J.; Lehtolahti, J.; Laukkanen, J.; Kuittinen, M.; Kauranen, M. Metamaterials with Tailored Nonlinear Optical Response. *Nano Lett.* **2012**, *12*, 673–677.
13. Castro-Lopez, M.; Brinks, D.; Sapienza, R.; van Hulst, N. F. Aluminum for Nonlinear Plasmonics: Resonance-Driven Polarized Luminescence of Al, Ag, and Au Nanoantennas. *Nano Lett.* **2011**, *11*, 4674–4678.
14. Biagioni, P.; Brida, D.; Huang, J.-S.; Kern, J.; Duò, L.; Hecht, B.; Finazzi, M.; Cerullo, G. Dynamics of Four-Photon Photoluminescence in Gold Nanoantennas. *Nano Lett.* **2012**, *12*, 2941–2947.
15. Ko, K. D.; Kumar, A.; Fung, K. H.; Ambekar, R.; Liu, G. L.; Fang, N. X.; Kimani, J.; Toussaint, C. Nonlinear Optical Response from Arrays of Au Bowtie Nanoantennas. *Nano Lett.* **2011**, *11*, 61–65.
16. Lippitz, M.; van Dijk, M. A.; Orrit, M. Third-Harmonic Generation from Single Gold Nanoparticles. *Nano Lett.* **2005**, *5*, 799–802.
17. Schwartz, O.; Oron, D. Background-Free Third Harmonic Imaging of Gold Nanorods. *Nano Lett.* **2009**, *9*, 4093–4097.
18. Hanke, T.; Cesar, J.; Knittel, V.; Trügler, A.; Hohenester, U.; Leitenstorfer, A.; Bratschitsch, R. Tailoring Spatialtemporal Light Confinement in Single Plasmonic Nanoantennas. *Nano Lett.* **2012**, *12*, 992–996.
19. Hentschel, M.; Utikal, T.; Giessen, H.; Lippitz, M. Quantitative Modeling of the Third Harmonic Emission Spectrum of Plasmonic Nanoantennas. *Nano Lett.* **2012**, *12*, 3778–3782.
20. Navarro-Cia, M.; Maier, S. A. Broad-Band Near-Infrared Plasmonic Nanoantennas for Higher Harmonic Generation. *ACS Nano* **2012**, *6*, 3537–3544.
21. Danckwerts, M.; Novotny, L. Optical Frequency Mixing at Coupled Gold Nanoparticles. *Phys. Rev. Lett.* **2007**, *98*, 026104.
22. Harutyunyan, H.; Volpe, G.; Quidant, R.; Novotny, L. Enhancing the Nonlinear Optical Response Using Multifrequency Gold-Nanowire Antennas. *Phys. Rev. Lett.* **2012**, *108*, 217403.
23. Loudon, R. *The Quantum Theory of Light*; Oxford University Press: Oxford, 2000.
24. Bloembergen, N.; Chang, R. K.; Jha, S. S.; Lee, C. H. Optical Second-Harmonic Generation in Reflection from Media with Inversion Symmetry. *Phys. Rev.* **1968**, *174*, 813.
25. Mizrahi, V.; Sipe, J. E. Phenomenological Treatment of Surface Second-Harmonic generation. *J. Opt. Soc. Am. B* **1988**, *5*, 660–667.
26. Shen, Y. R. Optical Second Harmonic Generation at Interfaces. *Annu. Rev. Phys. Chem.* **1989**, *40*, 327–350.
27. Shen, Y. R. Surface Properties Probed by Second-Harmonic and Sum-Frequency Generation. *Nature* **1989**, *337*, 519–525.
28. Wang, F. X.; Rodriguez, F. J.; Albers, W. M.; Ahorinta, R.; Sipe, J. E.; Kauranen, M. Surface and Bulk Contributions to the Second-Order Nonlinear Optical Response of a Gold Film. *Phys. Rev. B: Condens. Matter Mater. Phys.* **2009**, *80*, 233402.
29. Bachelier, G.; Butet, J.; Russier-Antoine, I.; Jonin, C.; Benichou, E.; Brevet, P.-F. Origin of Optical Second-Harmonic Generation in Spherical Gold Nanoparticles: Local Surface and Nonlocal Bulk Contributions. *Phys. Rev. B: Condens. Matter Mater. Phys.* **2010**, *82*, 235403.
30. Krause, D.; Teplin, C. W.; Rogers, C. T. Optical Surface Second Harmonic Measurements of Isotropic Thin-Film Metals: Gold, Silver, Copper, Aluminum, and Tantalum. *J. Appl. Phys.* **2004**, *96*, 3626.
31. Thyagarajan, K.; Rivier, S.; Lovera, A.; Martin, O. J. F. Enhanced Second-Harmonic Generation from Double Resonant Plasmonic Antennae. *Opt. Express* **2012**, *20*, 12860–12865.
32. Metzger, B.; Gui, L.; Fuchs, J.; Floess, D.; Hentschel, M.; Giessen, H. Strong Enhancement of Second Harmonic Emission by Plasmonic Resonances at the Second Harmonic Wavelength. *Nano Lett.* **2015**, *15*, 3917–3922.
33. Rudnick, J.; Stern, E. A. Second-Harmonic Radiation from Metal Surfaces. *Phys. Rev. B* **1971**, *4*, 4274.
34. Sipe, J. E.; So, V. C. Y.; Fukui, M.; Stegeman, G. I. Analysis of Second-Harmonic Generation at Metal Surfaces. *Phys. Rev. B: Condens. Matter Mater. Phys.* **1980**, *21*, 4389.
35. Zeng, Y.; Hoyer, W.; Liu, J. J.; Koch, S. W.; Moloney, J. V. Classical Theory for Second-Harmonic Generation from Metallic Nanoparticles. *Phys. Rev. B: Condens. Matter Mater. Phys.* **2009**, *79*, 235109.
36. Scalora, M.; Vincenti, M. A.; de Ceglia, D.; Roppo, V.; Centini, M.; Akozbek, N.; Bloemer, M. J. Second- and Third-Harmonic Generation in Metal-Based Structures. *Phys. Rev. A: At., Mol., Opt. Phys.* **2010**, *82*, 043828.
37. Vincenti, M. A.; de Ceglia, D.; Roppo, V.; Scalora, M. Harmonic Generation in Metallic, GaAs-Filled Nanocavities in the Enhanced Transmission Regime at Visible and UV Wavelengths. *Opt. Express* **2011**, *19*, 2064–2078.
38. Ciracì, C.; Poutrina, E.; Scalora, M.; Smith, D. R. Second-Harmonic Generation in Metallic Nanoparticles: Clarification of the Role of the Surface. *Phys. Rev. B: Condens. Matter Mater. Phys.* **2012**, *86*, 115451.
39. Ginzburg, P.; Krasavin, A. V.; Wurtz, G. A.; Zayats, A. V. Nonperturbative Hydrodynamic Model for Multiple Harmonics Generation in Metallic Nanostructures. *ACS Photonics* **2015**, *2*, 8–13.
40. Mäkitalo, J.; Suuriniemi, S.; Kauranen, M. Boundary Element Method for Surface Nonlinear Optics of Nanoparticles. *Opt. Express* **2011**, *19*, 23386–23399.
41. Forestiere, C.; Capretti, A.; Miano, G. Surface Integral Method for Second Harmonic Generation in Metal Nanoparticles Including Both Local-Surface and Nonlocal-Bulk Sources. *J. Opt. Soc. Am. B* **2013**, *30*, 2355–2364.
42. Guyot-Sionnest, P.; Shen, Y. R. Bulk Contribution in Surface Second-Harmonic Generation. *Phys. Rev. B: Condens. Matter Mater. Phys.* **1988**, *38*, 7985.
43. O'Donnell, K. A.; Torre, R. Characterization of the Second-Harmonic Response of a Silver-Air Interface. *New J. Phys.* **2005**, *7*, 154.
44. Luce, T. A.; Hubner, W.; Bennemann, K. H. Theory for the Nonlinear Optical Response at Noble-Metal Surfaces with Nonequilibrium Electrons. *Z. Phys. B: Condens. Matter* **1997**, *102*, 223–232.
45. Liebsch, A. Second-Harmonic Generation at Simple Metal Surfaces. *Phys. Rev. Lett.* **1988**, *61*, 1233.
46. Schaich, W. L. Calculations of Second-Harmonic Generation for a Jellium Metal Surface. *Phys. Rev. B: Condens. Matter Mater. Phys.* **2000**, *61*, 10478.
47. Scalora, M.; Vincenti, M. A.; de Ceglia, D.; Haus, J. W. Nonlocal and Quantum-Tunneling Contributions to Harmonic Generation in Nanostructures: Electron-Cloud-Screening Effects. *Phys. Rev. A: At., Mol., Opt. Phys.* **2014**, *90*, 013831.
48. Haus, J. W.; de Ceglia, D.; Vincenti, M. A.; Scalora, M. Nonlinear Quantum Tunneling Effects in Nanoplasmonic Environments: Two-Photon Absorption and Harmonic Generation. *J. Opt. Soc. Am. B* **2014**, *31*, A13–A19.
49. Hao, E. C.; Schatz, G. C.; Johnson, R. C.; Hupp, J. T. Hyper-Rayleigh Scattering from Silver Nanoparticles. *J. Chem. Phys.* **2002**, *117*, 5963–5966.
50. Nappa, J.; Russier-Antoine, I.; Benichou, E.; Jonin, C.; Brevet, P.-F. Second Harmonic Generation from Small

Gold Metallic Particles: From the Dipolar to the Quadrupolar Response. *J. Chem. Phys.* **2006**, *125*, 184712.
51. Russier-Antoine, I.; Benichou, E.; Bachelier, G.; Jonin, C.; Brevet, P.-F. Multipolar Contributions of the Second Harmonic Generation from Silver and Gold Nanoparticles. *J. Phys. Chem. C* **2007**, *111*, 9044.
52. Chandra, M.; Das, P. K. Size Dependence and Dispersion Behavior of the First Hyperpolarizability of Copper Nanoparticles. *Chem. Phys. Lett.* **2009**, *476*, 62–64.
53. Gonella, G.; Gan, W.; Xu, B.; Dai, H.-L. The Effect of Composition, Morphology, and Susceptibility on Nonlinear Light Scattering from Metallic and Dielectric Nanoparticles. *J. Phys. Chem. Lett.* **2012**, *3*, 2877–2881.
54. Capretti, A.; Pecora, E. F.; Forestiere, C.; Dal Negro, L.; Miano, G. Size-Dependent Second-Harmonic Generation from Gold Nanoparticles. *Phys. Rev. B: Condens. Matter Mater. Phys.* **2014**, *89*, 125414.
55. Nappa, J.; Revillod, G.; Abid, J.-P.; Russier-Antoine, I.; Jonin, C.; Benichou, E.; Girault, H.; Brevet, P.-F. Hyper-Rayleigh Scattering of Gold Nanorods and Their Relationship with Linear Assemblies of Gold Nanospheres. *Faraday Discuss.* **2004**, *125*, 145.
56. Hubert, C.; Billot, L.; Adam, P.-M.; Bachelot, R.; Royer, P.; Grand, J.; Gindre, D.; Dorkenoo, K. D.; Fort, A. Role of Surface Plasmon in Second Harmonic Generation from Gold Nanorods. *Appl. Phys. Lett.* **2007**, *90*, 181105.
57. Singh, A.; Lehoux, A.; Remita, H.; Zyss, J.; Ledoux-Rak, I. Second Harmonic Response of Gold Nanorods: A Strong Enhancement with the Aspect Ratio. *J. Phys. Chem. Lett.* **2013**, *4*, 3958–3961.
58. El Harfouch, Y.; Benichou, E.; Bertorelle, F.; Russier-Antoine, I.; Jonin, C.; Lascoux, N.; Brevet, P.-F. Hyper-Rayleigh Scattering from Gold Nanorods. *J. Phys. Chem. C* **2014**, *118*, 609–616.
59. Hasan, S.-B.; Etrich, C.; Filter, R.; Rockstuhl, C.; Lederer, F. Enhancing the Nonlinear Response of Plasmonic Nanowire Antennas by Engineering their Terminations. *Phys. Rev. B: Condens. Matter Mater. Phys.* **2013**, *88*, 205125.
60. Senapati, D.; Singh, A. K.; Khan, S. A.; Senapati, T.; Ray, C. P. Probing Real Time Gold Nanostar Formation Process using Two-Photon Scattering Spectroscopy. *Chem. Phys. Lett.* **2011**, *504*, 46–51.
61. Singh, A. K.; Senapati, D.; Neely, A.; Kolawole, G.; Hawker, C.; Ray, C. P. Nonlinear Optical Properties of Triangular Silver Nanomaterials. *Chem. Phys. Lett.* **2009**, *481*, 94–98.
62. Schön, P.; Bonod, N.; Devaux, E.; Wenger, J.; Rigneault, H.; Ebbesen, T. W.; Brasselet, S. Enhanced Second-Harmonic Generation from Individual Metallic Nanoapertures. *Opt. Lett.* **2010**, *35*, 4063–4065.
63. Xu, T.; Jiao, X.; Zhang, G.-P.; Blair, S. Second-Harmonic Emission from Sub-Wavelength Apertures: Effects of Aperture Symmetry and Lattice Arrangement. *Opt. Express* **2007**, *15*, 13894–13906.
64. Salomon, A.; Zielinski, M.; Kolkowski, R.; Zyss, J.; Prior, Y. ize and Shape Resonances in Second Harmonic Generation from Silver Nanocavities. *J. Phys. Chem. C* **2013**, *117*, 22377–22382.
65. Kolkowski, R.; Szeszko, J.; Dwir, B.; Kapon, E.; Zyss, J. Effects of Surface Plasmon Polariton-Mediated Interactions on Second Harmonic Generation from Assemblies of Pyramidal Metallic Nano-Cavities. *Opt. Express* **2014**, *22*, 30592–30606.
66. Kim, M.-K.; Sim, H.; Yoon, S. J.; Gong, S.-H.; Ahn, C. W.; Cho, Y.-H.; Lee, Y.-H. Squeezing Photons into a Point-Like Space. *Nano Lett.* **2015**, *15*, 4102–4107.
67. Belardini, A.; Larciprete, M. C.; Centini, M.; Fazio, E.; Sibilia, C. Circular Dichroism in the Optical Second-Harmonic Emission of Curved Gold Metal Nanowires. *Phys. Rev. Lett.* **2011**, *107*, 257401.
68. Klein, M. W.; Enkrich, C.; Wegener, M.; Linden, S. Second-Harmonic Generation from Magnetic Metamaterials. *Science* **2006**, *313*, 502–504.
69. Ciracì, C.; Poutrina, E.; Scalora, M.; Smith, D. R. Origin of second-harmonic generation enhancement in optical split-ring resonators. *Phys. Rev. B: Condens. Matter Mater. Phys.* **2012**, *85*, 201403(R).
70. Linden, S.; Niesler, F. B. P.; Förstner, J.; Grynko, Y.; Meier, T.; Wegener, M. Collective Effects in Second-Harmonic Generation from Split-Ring-Resonator Arrays. *Phys. Rev. Lett.* **2012**, *109*, 015502.
71. Kruk, S.; Weismann, M.; Bykov, A. Y.; Mamonov, E. A.; Kolmychek, I. A.; Murzina, T.; Panoiu, N. C.; Neshev, D. N.; Kivshar, Y. S. Enhanced Magnetic Second-Harmonic Generation from Resonant Metasurfaces. *ACS Photonics* **2015**, *2*, 1007–1012.
72. Canfield, B. K.; Husu, H.; Laukkanen, J.; Bai, B. F.; Kuittinen, M.; Turunen, J.; Kauranen, M. Local Field Asymmetry Drives Second-Harmonic Generation in Noncentrosymmetric Nanodimers. *Nano Lett.* **2007**, *7*, 1251–1255.
73. Valev, V. K.; Smisdom, N.; Silhanek, A. V.; De Clercq, B.; Gillijns, W.; Ameloot, M.; Moshchalkov, V. V.; Verbiest, T. Plasmonic Ratchet Wheels: Switching Circular Dichroism by Arranging Chiral Nanostructures. *Nano Lett.* **2009**, *9*, 3945–3948.
74. Valev, V. K.; Volodin, A.; Silhanek, A. V.; Gillijns, W.; De Clercq, B.; Jeyaram, Y.; Paddubrouskaya, H.; Biris, C. G.; Panoiu, N. C.; Aktsipetrov, O. A.; et al. Plasmons Reveal the Direction of Magnetization in NickelN. *ACS Nano* **2011**, *5*, 91–96.
75. Valev, V. K. Characterization of Nanostructured Plasmonic Surfaces with Second Harmonic Generation. *Langmuir* **2012**, *28*, 15454–15471.
76. Mamonov, E. A.; Kolmychek, I. A.; Vandendriessche, S.; Hojeij, M.; Ekinci, Y.; Valev, V. K.; Verbiest, T.; Murzina, T. V. Anisotropy Versus Circular Dichroism in Second Harmonic Generation from Fourfold Symmetric Arrays of G-Shaped Nanostructures. *Phys. Rev. B: Condens. Matter Mater. Phys.* **2014**, *89*, 121113(R).
77. Valev, V. K.; Baumberg, J. J.; Sibilia, C.; Verbiest, T. Chirality and Chiroptical Effects in Plasmonic Nanostructures: Fundamentals, Recent Progress, and Outlook. *Adv. Mater.* **2013**, *25*, 2517–2534.
78. Valev, V. K.; Silhanek, A. V.; Verellen, N.; Gillijns, W.; Van Dorpe, P.; Aktsipetrov, O. A.; Vandenbosch, G. A. E.; Moshchalkov, V. V.; Verbiest, T. Asymmetric Optical Second-Harmonic Generation from Chiral G-Shaped Gold Nanostructures. *Phys. Rev. Lett.* **2010**, *104*, 127401.
79. Valev, V. K.; De Clercq, B.; Zheng, X.; Denkova, D.; Osley, E. J.; Vandendriessche, S.; Silhanek, A. V.; Volskiy, V.; Warburton, P. A.; Vandenbosch, G. A. E.; et al. The Role of Chiral Local Field Enhancements Below the Resolution Limit of Second Harmonic Generation Microscopy. *Opt. Express* **2012**, *20*, 256–264.
80. Decker, M.; Ruther, M.; Kriegler, C. E.; Zhou, J.; Soukoulis, C. M.; Linden, S.; Wegener, M. Strong Optical Activity from Twisted-Cross Photonic Metamaterials. *Opt. Lett.* **2009**, *34*, 2501.
81. Huttunen, M. J.; Bautista, G.; Decker, M.; Linden, S.; Wegener, M.; Kauranen, M. Nonlinear Chiral Imaging of Subwavelength-Sized Twisted-Cross Gold Nanodimers [Invited]. *Opt. Mater. Express* **2011**, *1*, 46–56.
82. Kujala, S.; Canfield, B. K.; Kauranen, M.; Svirko, Y.; Turunen, J. Multipole Interference in the Second-Harmonic Optical Radiation from Gold Nanoparticles. *Phys. Rev. Lett.* **2007**, *98*, 167403.
83. Canfield, B. K.; Kujala, S.; Jefimovs, K.; Svirko, Y.; Turunen, J.; Kauranen, M. A Macroscopic Formalism to Describe the Second-Order Nonlinear Optical Response of Nanostructures. *J. Opt. A: Pure Appl. Opt.* **2006**, *8*, S278–S284.
84. Czaplicki, R.; Zdanowicz, M.; Koskinen, K.; Laukkanen, J.; Kuittinen, M.; Kauranen, M. Dipole Limit in Second-Harmonic Generation from Arrays of Gold Nanoparticles. *Opt. Express* **2011**, *19*, 26866–26871.
85. Kujala, S.; Canfield, B. K.; Kauranen, M.; Svirko, Y.; Turunen, J. Multipolar Analysis of Second-Harmonic Radiation from Gold Nanoparticles. *Opt. Express* **2008**, *16*, 17196–17208.
86. Neacsu, C. C.; Reider, G. A.; Raschke, M. B. Second-Harmonic Generation from Nanoscopic Metal Tips: Symmetry Selection Rules for Single Asymmetric Nanostructures.

Phys. Rev. B: Condens. Matter Mater. Phys. **2005**, *71*, 201402(R).
87. Anderson, A.; Deryckx, K. S.; Xu, X. G.; Steinmeyer, G.; Raschke, M. B. Few-Femtosecond Plasmon Dephasing of a Single Metallic Nanostructure from Optical Response Function Reconstruction by Interferometric Frequency Resolved Optical Gating. *Nano Lett.* **2010**, *10*, 2519–2524.
88. Reichenbach, P.; Horneber, A.; Gollmer, D. A.; Hille, A.; Mihaljevic, J.; Schäfer, C.; Kern, D. P.; Meixner, A. J.; Zhang, D.; Fleischer, M.; et al. Nonlinear Optical Point Light Sources Through Field Enhancement at Metallic Nanocones. *Opt. Express* **2014**, *22*, 15484–15501.
89. Bertolotti, M.; Belardini, A.; Benedetti, A.; Sibilia, C. Second Harmonic Circular Dichroism by Self-Assembled Metasurfaces [Invited]. *J. Opt. Soc. Am. B* **2015**, *32*, 1287–1293.
90. Kolkowski, R.; Petti, L.; Rippa, M.; Lafargue, C.; Zyss, J. Octupolar Plasmonic Meta-Molecules for Nonlinear Chiral Watermarking at Subwavelength Scale. *ACS Photonics* **2015**, *2*, 899–906.
91. Valev, V. K.; Baumberg, J. J.; de Clercq, B.; Braz, N.; Zheng, X.; Osley, E. J.; Vandendriessche, S.; Hojeij, M.; Blejean, C.; Mertens, J.; et al. Nonlinear Superchiral Meta-Surfaces: Tuning Chirality and Disentangling Non-Reciprocity at the Nanoscale. *Adv. Mater.* **2014**, *26*, 4074–4081.
92. van Nieuwstadt, J. A. H.; sandtke, M.; Harmsen, R. H.; Segerink, F. B.; Prangsma, J. C.; Enoch, S.; Kuipers, L. Strong Modification of the Nonlinear Optical Response of Metallic Subwavelength Hole Arrays. *Phys. Rev. Lett.* **2006**, *97*, 146102.
93. Russier-Antoine, I.; Duboisset, J.; Bachelier, G.; Benichou, E.; Jonin, C.; Del Fatti, N.; Vallée, F.; Sánchez-Iglesias, A.; Pastoriza-Santos, I.; Liz-Marzan, L. M.; et al. Symmetry Cancellations in the Quadratic Hyperpolarizability of Non-Centrosymmetric Gold Decahedra. *J. Phys. Chem. Lett.* **2010**, *1*, 874.
94. Finazzi, M.; Biagioni, P.; Celebrano, M.; Duò, L. Selection Rules for Second-Harmonic Generation in Nanoparticles. *Phys. Rev. B: Condens. Matter Mater. Phys.* **2007**, *76*, 125414.
95. Butet, J.; Dutta-Gupta, S.; Martin, O. J. F. Surface Second-Harmonic Generation from Coupled Spherical Plasmonic Nanoparticles: Eigenmode Analysis and Symmetry Properties. *Phys. Rev. B: Condens. Matter Mater. Phys.* **2014**, *89*, 245449.
96. Benedetti, A.; Centini, M.; Bertolotti, M.; Sibilia, C. Second Harmonic Generation from 3D Nanoantennas: On the Surface and Bulk Contributions by Far-Field Pattern Analysis. *Opt. Express* **2011**, *19*, 26752–26727.
97. Kottmann, J. P.; Martin, O. J. F. Plasmon Resonant Coupling in Metallic Nanowires. *Opt. Express* **2001**, *8*, 655–663.
98. Berthelot, J.; Bachelier, G.; Song, M.; Rai, P.; Colas des Francs, G.; Dereux, A.; Bouhelier, A. Silencing and Enhancement of Second-Harmonic Generation in Optical Gap Antennas. *Opt. Express* **2012**, *20*, 10498–10508.
99. Slablab, A.; Le Xuan, L.; Zielinski, M.; de Wilde, Y.; Jacques, V.; Chauvat, D.; Roch, J.-F. Second-Harmonic Generation from Coupled Plasmon Modes in a Single Dimer of Gold Nanospheres. *Opt. Express* **2012**, *20*, 220–227.
100. de Ceglia, D.; Vincenti, M. A.; de Angelis, C.; Locatelli, A.; Haus, J. W.; Scalora, M. Role of Antenna Modes and Field Enhancement in Second Harmonic Generation from Dipole Nanoantenna. *Opt. Express* **2015**, *23*, 1715–1729.
101. Biswas, S.; Liu, X.; Jarrett, J. W.; Brown, D.; Pustovit, V.; Urbas, A.; Knappenberger, K. L., Jr.; Nealey, P. F.; Vaia, R. A. Nonlinear Chiro-Optical Amplification by Plasmonic Nanolens Arrays Formed via Directed Assembly of Gold Nanoparticles. *Nano Lett.* **2015**, *15*, 1836–1842.
102. Nappa, J.; Revillod, G.; Russier-Antoine, I.; Benichou, E.; Jonin, C.; Brevet, P. F. Electric Dipole Origin of the Second Harmonic Generation of Small Metallic Particles. *Phys. Rev. B: Condens. Matter Mater. Phys.* **2005**, *71*, 165407.
103. Simon, H. J.; Mitchell, D. E.; Watson, J. G. Optical Second-Harmonic Generation with Surface Plasmons in Silver Films. *Phys. Rev. Lett.* **1974**, *33*, 1531–1534.
104. Agarwal, G. S.; Jha, S. S. Theory of Second Harmonic Generation at a Metal Surface with Surface Plasmon Excitation. *Solid State Commun.* **1982**, *41*, 499–501.
105. Hua, X. M.; Gersten, J. I. Theory of Second-Harmonic Generation by Small Metal Spheres. *Phys. Rev. B: Condens. Matter Mater. Phys.* **1986**, *33*, 3756.
106. Vance, F. W.; Lemon, B. I.; Hupp, J. T. Enormous Hyper-Rayleigh Scattering from Nanocrystalline Gold Particle Suspensions. *J. Phys. Chem. B* **1998**, *102*, 10091–10093.
107. Staedler, D.; Magouroux, T.; Hadji, R.; Joulaud, C.; Extermann, J.; Schwung, S.; Passemard, S.; Kasparian, C.; Clarke, G.; Gerrmann, M.; et al. Harmonic Nanocrystals for Biolabeling: A Survey of Optical Properties and Biocompatibility. *ACS Nano* **2012**, *6*, 2542–2549.
108. Dadap, J. I.; Shan, J.; Eisenthal, K. B.; Heinz, T. F. Second-Harmonic Rayleigh Scattering from a Sphere of Centrosymmetric Material. *Phys. Rev. Lett.* **1999**, *83*, 4045–4048.
109. Dadap, J. I.; Shan, J.; Heinz, T. F. Theory of Optical Second-Harmonic Generation from a Sphere of Centrosymmetric Material: Small-Particle Limit. *J. Opt. Soc. Am. B* **2004**, *21*, 1328.
110. Luk'yanchuk, B.; Zheludev, N. I.; Maier, S. A.; Halas, N. J.; Nordlander, P.; Giessen, H.; Chong, C. T. The Fano Resonance in Plasmonic Nanostructures and Metamaterials. *Nat. Mater.* **2010**, *9*, 707–715.
111. Miroshnichenko, A. E.; Flach, S.; Kivshar, Y. S. Fano Resonances in Nanoscale Structures. *Rev. Mod. Phys.* **2010**, *82*, 2257–2298.
112. Hao, F.; Nordlander, P.; Sonnefraud, Y.; Van Dorpe, P.; Maier, S. A. Tunability of Subradiant Dipolar and Fano-Type Plasmon Resonances in Metallic Ring/Disk Cavities: Implications for Nanoscale Optical Sensing. *ACS Nano* **2009**, *3*, 643–652.
113. Fu, Y. H.; Zhang, J. B.; Yu, Y. F.; Luk'yanchuk, B. Generating and Manipulating Higher Order Fano Resonances in Dual-Disk Ring Plasmonic Nanostructures. *ACS Nano* **2012**, *6*, 5130–5137.
114. Cetin, A. E.; Altug, H. Fano Resonant Ring/Disk Nanocavities on Conducting Substrates for Advanced Biosensing. *ACS Nano* **2012**, *6*, 9989–9995.
115. Verellen, N.; Sonnefraud, Y.; Sobhani, H.; Hao, F.; Moshchalkov, V. V.; Van Dorpe, P.; Nordlander, P.; Maier, S. A. Fano Resonances in Individual Coherent Plasmonic Nanocavities. *Nano Lett.* **2009**, *9*, 1663–1667.
116. Liu, N.; Weiss, T.; Mesch, M.; Langguth, L.; Eigenthaler, U.; Hirscher, M.; Soennichsen, C.; Giessen, H. Planar Metamaterial Analogue of Electromagnetically Induced Transparency for Plasmonic Sensing. *Nano Lett.* **2010**, *10*, 1103–1107.
117. Lassiter, J. B.; Sobhani, H.; Fan, J. A.; Kundu, J.; Capasso, F.; Nordlander, P.; Halas, N. J. Fano Resonances in Plasmonic Nanoclusters: Geometrical and Chemical Tunability. *Nano Lett.* **2010**, *10*, 3184–3189.
118. Hentschel, M.; Saliba, M.; Vogelgesang, R.; Giessen, H.; Alivisatos, A. P.; Liu, N. Transition from Isolated to Collective Modes in Plasmonic Oligomers. *Nano Lett.* **2010**, *10*, 2721–2726.
119. Hentschel, M.; Dregely, D.; Vogelgesang, R.; Giessen, H.; Liu, N. Plasmonic Oligomers: The Role of Individual Particles in Collective Behavior. *ACS Nano* **2011**, *5*, 2042–2050.
120. Gallinet, B.; Martin, O. J. F. Influence of Electromagnetic Interactions on the Line Shape of Plasmonic Fano Resonances. *ACS Nano* **2011**, *5*, 8999–9008.
121. Giannini, V.; Francescato, Y.; Amrania, H.; Phillips, C. C.; Maier, S. A. Fano Resonances in Nanoscale Plasmonic Systems: A Parameter-Free Modeling Approach. *Nano Lett.* **2011**, *11*, 2835–2840.
122. Rahmani, M.; Lei, D. Y.; Giannini, V.; Lukiyanchuk, B.; Ranjbar, M.; Liew, T. Y. F.; Hong, M.; Maier, S. A. Subgroup Decomposition of Plasmonic Resonances in Hybrid Oligomers: Modeling the Resonance Lineshape. *Nano Lett.* **2012**, *12*, 2101–2106.
123. Butet, J.; Martin, O. J. F. Nonlinear Plasmonic Nanorulers. *ACS Nano* **2014**, *8*, 4931–4939.

124. Butet, J.; Martin, O. J. F. Refractive Index Sensing with Fano Resonant Plasmonic Nanostructures: A Symmetry Based Nonlinear Approach. *Nanoscale* **2014**, *6*, 15262–15270.
125. Knight, M. W.; King, N. S.; Liu, L.; Everitt, H. O.; Nordlander, P.; Halas, N. J. Aluminum for Plasmonics. *ACS Nano* **2014**, *8*, 834–840.
126. Aouani, H.; Navarro-Cia, M.; Rahmani, M.; Sidiropoulos, T. P. H.; Hong, M.; Oulton, R. F.; Maier, S. A. Multiresonant Broadband Optical Antennas As Efficient Tunable Nanosources of Second Harmonic Light. *Nano Lett.* **2012**, *12*, 4997–5002.
127. Celebrano, M.; Wu, X.; Baselli, M.; Groβmann, S.; Biagioni, P.; Locatelli, A.; De Angelis, C.; Cerullo, G.; Osellame, R.; Hecht, B.; et al. Mode Matching in Multiresonant Plasmonic Nanoantennas for Enhanced Second Harmonic Generation. *Nat. Nanotechnol.* **2015**, *10*, 412–417.
128. Butet, J.; Martin, O. J. F. Fano Resonances in the Nonlinear Optical response of Coupled Plasmonic Nanostructures. *Opt. Express* **2014**, *22*, 29693–29707.
129. Thyagarajan, K.; Butet, J.; Martin, O. J. F. Augmenting Second Harmonic Generation Using Fano Resonances in Plasmonic Systems. *Nano Lett.* **2013**, *13*, 1847–1851.
130. Walsh, G. F.; Dal Negro, L. Enhanced Second Harmonic Generation by Photonic-Plasmonics Fano-Type Coupling in Nanoplasmonic Arrays. *Nano Lett.* **2013**, *13*, 3111–3117.
131. Czaplicki, R.; Husu, H.; Siikanen, R.; Mäkitalo, J.; Kauranen, M. Enhancement of Second-Harmonic Generation from Metal Nanoparticles by Passive Elements. *Phys. Rev. Lett.* **2013**, *110*, 093902.
132. Lehr, D.; Reinhold, J.; Thiele, I.; Hartung, H.; Dietrich, K.; Menzel, C.; Pertsch, T.; Kley, E.-B.; Tünnermann, A. Enhancing Second Harmonic Generation in Gold Nanoring Resonators Filled with Lithium Niobate. *Nano Lett.* **2015**, *15*, 1025–1030.
133. Chen, P.-Y.; Argyropoulos, C.; D'Aguanno, G.; Alù, A. Enhanced Second-Harmonic Generation by Metasurface Nanomixer and Nanocavity. *ACS Photonics* **2015**, *2*, 1000–1006.
134. Pu, Y.; Grange, R.; Hsieh, C. L.; Psaltis, D. Nonlinear Optical Properties of Core-Shell Nanocavities for Enhanced Second-Harmonic Generation. *Phys. Rev. Lett.* **2010**, *104*, 207402.
135. Arbouet, A.; Christofilos, D.; Del Fatti, N.; Vallée, F.; Huntzinger, J.-R.; Arnaud, L.; Billaud, P.; Broyer, M. Direct Measurement of the Single-Metal-Cluster Optical Absorption. *Phys. Rev. Lett.* **2004**, *93*, 127401.
136. Olson, J.; Dominguez-Medina, S.; Hoggard, A.; Wang, L.-Y.; Chang, W.-S.; Link, S. Optical Characterization of Single Plasmonic Nanoparticles. *Chem. Soc. Rev.* **2015**, *44*, 40–57.
137. Zijlstra, P.; Orrit, M. Single Metal Nanoparticles: Optical Detection, Spectroscopy and Applications. *Rep. Prog. Phys.* **2011**, *74*, 106401.
138. Jin, R.; Jureller, J. E.; Kim, H. Y.; Scherer, N. F. Correlating Second Harmonic Optical Responses of Single Ag Nanoparticles with Morphology. *J. Am. Chem. Soc.* **2005**, *127*, 12482.
139. Butet, J.; Bachelier, G.; Duboisset, J.; Bertorelle, F.; Russier-Antoine, I.; Jonin, C.; Benichou, E.; Brevet, P.-F. Three-Dimensionnal Mapping of Single Gold Nanoparticles Embedded in a Homogeneous Transparent Matrix using Optical Second-Harmonic Generation. *Opt. Express* **2010**, *18*, 22314.
140. Duboisset, J.; Russier-Antoine, I.; Benichou, E.; Bachelier, G.; Jonin, C.; Brevet, P.-F. Single Metallic Nanoparticle Sensitivity with Hyper Rayleigh Scattering. *J. Phys. Chem. C* **2009**, *113*, 13477.
141. Zavelani-Rossi, M.; Celebrano, M.; Biagioni, P.; Polli, D.; Finazzi, M.; Duò, L.; Cerullo, G.; Labardi, M.; Allegrini, M.; Grand, J.; Adam, P.-M. Near-Field Second-Harmonic Generation in Single Gold Nanoparticles. *Appl. Phys. Lett.* **2008**, *92*, 093119.
142. Bachelier, G.; Russier-Antoine, I.; Benichou, E.; Jonin, C.; Brevet, P.-F. Multipolar Second-Harmonic Generation in Noble Metal Nanoparticles. *J. Opt. Soc. Am. B* **2008**, *25*, 955–960.
143. O'Donnell, K. A.; Torre, R. Second-Harmonic Generation from a Strongly Rough Metal Surface. *Opt. Commun.* **1997**, *138*, 341–344.
144. Stockman, M. I.; Bergman, D. J.; Anceau, C.; Brasselet, S.; Zyss, J. Enhanced Second-Harmonic Generation by Metal Surfaces with Nanoscale Roughness: Nanoscale Dephasing, Depolarization, and Correlations. *Phys. Rev. Lett.* **2004**, *92*, 057402.
145. Butet, J.; Thyagarajan, K.; Martin, O. J. F. Ultrasensitive Optical Shape Characterization of Gold Nanoantennas Using Second Harmonic Generation. *Nano Lett.* **2013**, *13*, 1787–1792.
146. Kern, A. M.; Martin, O. J. F. Excitation and Reemission of Molecules near Realistic Plasmonic Nanostructures. *Nano Lett.* **2011**, *11*, 482–487.
147. Bautista, G.; Huttunen, M. J.; Mäkitalo, J.; Kontio, J. M.; Simonen, J.; Kauranen, M. Second-Harmonic Generation Imaging of Metal Nano-Objects with Cylindrical Vector Beams. *Nano Lett.* **2012**, *12*, 3207–3212.
148. Liz-Marzán, L. M. Tailoring Surface Plasmons through the Morphology and Assembly of Metal Nanoparticles. *Langmuir* **2006**, *22*, 32–41.
149. Eustis, S.; El-Sayed, M. A. Why Gold Nanoparticles Are More Precious Than Pretty Gold: Noble Metal Surface Plasmon Resonance and its Enhancement of the Radiative and Nonradiative Properties of Nanocrystals of Different Shapes. *Chem. Soc. Rev.* **2006**, *35*, 209–217.
150. Sauerbeck, C.; Haderlein, M.; Schürer, B.; Braunschweig, B.; Peukert, W.; Taylor, R. N. K. Shedding Light on the Growth of Gold Nanoshells. *ACS Nano* **2014**, *8*, 3088–3096.
151. Russier-Antoine, I.; Huang, J.; Benichou, E.; Bachelier, G.; Jonin, C.; Brevet, P.-F. Hyper Rayleigh Scattering of Protein-Mediated Gold Nanoparticles Aggregates. *Chem. Phys. Lett.* **2008**, *450*, 345.
152. Nordlander, P.; Oubre, C.; Prodan, E.; Li, K.; Stockman, M. I. Plasmon Hybridization in Nanoparticle Dimers. *Nano Lett.* **2004**, *4*, 899–903.
153. Jain, P. K.; Huang, W.; El-Sayed, M. A. On the Universal Scaling Behavior of the Distance Decay of Plasmon Coupling in Metal Nanoparticle Pairs: A Plasmon Ruler Equation. *Nano Lett.* **2007**, *7*, 2080–2088.
154. Sonnichsen, C.; Reinhard, B. M.; Liphardt, J.; Alivisatos, A. P. A Molecular Ruler Based on Plasmon Coupling of Single Gold and Silver Nanoparticles. *Nat. Biotechnol.* **2005**, *23*, 741–745.
155. Wang, J.; Boriskina, S. V.; Wang, H.; Reinhard, B. M. Illuminating Epidermal Growth Factor Receptor Densities on Filopodia through Plasmon Coupling. *ACS Nano* **2011**, *5*, 6619–6628.
156. Yang, L.; Wang, H.; Yan, B.; Reinhard, B. M. Calibration of Silver Plasmon Rulers in 1−25 nm Separation Range: Experimental Indications of Distinct Plasmon Coupling Regimes. *J. Phys. Chem. C* **2010**, *114*, 4901–4908.
157. Anker, J. N.; Hall, W. P.; Lyandres, O.; Shah, N. C.; Zhao, J.; Van Duyne, R. P. Biosensing with Plasmonic Nanosensors. *Nat. Mater.* **2008**, *7*, 442–452.
158. Liu, N.; Hentschel, M.; Weiss, T.; Alivisatos, A. P.; Giessen, H. Three-Dimensional Plasmon Rulers. *Science* **2011**, *332*, 1407–1410.
159. Bouhelier, A.; Beversluis, M.; Hartschuh, A.; Novotny, L. Near-Field Second-Harmonic Generation Induced by Local Field Enhancement. *Phys. Rev. Lett.* **2003**, *90*, 013903.
160. Accanto, N.; Nieder, J. B.; Piatkowski, L.; Castro-Lopez, M.; Pastorelli, F.; Brinks, D.; van Hulst, N. F. Phase Control of Femtosecond Pulses on the Nanoscale using Second Harmonic Nanoparticles. *Light: Sci. Appl.* **2014**, *3*, e143.
161. Accanto, N.; Piatkowski, L.; Renger, J.; van Hulst, N. F. Capturing the Optical Phase Response of Nanoantennas by Coherent Second-Harmonic Microscopy. *Nano Lett.* **2014**, *14*, 4078–4082.
162. Lakowicz, J. R. Radiative Decay Engineering: Biophysical and Biomedical Applications. *Anal. Biochem.* **2001**, *298*, 1–24.

163. Anker, J. N.; Hall, W. P.; Lyandres, O.; Shah, N. C.; Zhao, J.; Van Duyne, R. P. Biosensing with plasmonic nanosensors. *Nat. Mater.* **2008**, *7*, 442–452.
164. Mayer, K. M.; Hafner, J. H. Localized Surface Plasmon Resonance Sensors. *Chem. Rev.* **2011**, *111*, 3828–3857.
165. Liu, N.; Tang, M. L.; Hentschel, M.; Giessen, H.; Alivisatos, A. P. Nanoantenna-enhanced gas sensing in a single tailored nanofocus. *Nat. Mater.* **2011**, *10*, 631.
166. Mock, J. J.; Smith, D. R.; Schultz, S. Local Refractive Index Dependence of Plasmon Resonance Spectra from Individual Nanoparticles. *Nano Lett.* **2003**, *3*, 485–491.
167. McFarland, A. D.; van Duyne, R. P. Single Silver Nanoparticles as Real-Time Optical Sensors with Zeptomole Sensitivity. *Nano Lett.* **2003**, *3*, 1057–1062.
168. Raschke, G.; Kowarik, S.; Franzl, T.; Soennichsen, C.; Klar, T. A.; Feldmann, J. Biomolecular Recognition Based on Single Gold Nanoparticle Light Scattering. *Nano Lett.* **2003**, *3*, 935–938.
169. Acimovic, S. S.; Kreuzer, M. P.; Gonzalez, M. U.; Quidant, R. Plasmon Near-Field Coupling in Metal Dimers as a Step toward Single-Molecule Sensing. *ACS Nano* **2009**, *3*, 1231–1237.
170. Ray, P. C. Size and Shape Dependent Second Order Nonlinear Optical Properties of Nanomaterials and their Application in Biological and Chemical Sensing. *Chem. Rev.* **2010**, *110*, 5332–5365.
171. Kim, Y.; Johnson, R. C.; Hupp, J. T. Gold Nanoparticle-Based Sensing of "Spectroscopically Silent" Heavy Metal Ions. *Nano Lett.* **2001**, *1*, 165–167.
172. Ray, P. C. Diagnostics of Single Base-Mismatch DNA Hybridization on Gold Nanoparticles by Using the Hyper-Rayleigh Scattering Technique. *Angew. Chem., Int. Ed.* **2006**, *45*, 1151–1154.
173. Singh, A. K.; Senapati, D.; Wang, S.; Griffin, J.; Neely, A.; Candice, P.; Naylor, K. M.; Varisli, B.; Kalluri, J. R.; Ray, P. C. Gold Nanorod Based Selective Identification of Escherichia coli Bacteria Using Two-Photon Rayleigh Scattering Spectroscopy. *ACS Nano* **2009**, *3*, 1906–1912.
174. Neely, A.; Perry, C.; Varisli, B.; Singh, A.; Arbneshi, T.; Senapati, D.; Kalluri, J. R.; Ray, P. C. Ultrasensitive and Highly Selective Detection of Alzheimer's Disease Biomarker Using Two-Photon Rayleigh Scattering Properties of Gold Nanoparticle. *ACS Nano* **2009**, *3*, 2834–2840.
175. Lu, W.; Arumugam, S. R.; Senapati, D.; Singh, A. K.; Arbneshi, T.; Khan, S. A.; Yu, H.; Ray, P. C. Multifunctional Oval Shape Gold Nanoparticle Based Selective Detection of Breast Cancer Cells Using Simple Colorimetric and Highly Sensitive Two-Photon Scattering. *ACS Nano* **2010**, *4*, 1739–1749.
176. Cao, Y. W. C.; Jin, R. C.; Mirkin, C. A. Nanoparticles with Raman Spectroscopic Fingerprints for DNA and RNA Detection. *Science* **2002**, *297*, 1536.
177. Abe, A.; Inoue, K.; Tanaka, T.; Kato, J.; Kajiyama, N.; Kawaguchi, R.; Tanaka, S.; Yoshiba, M.; Kohara, M. Quantitation of Hepatitis B Virus Genomic DNA by Real-Time Detection PCR. *J. Clin. Microbiol.* **1999**, *37*, 2899.
178. Darbha, G. K.; Ray, A.; Ray, P. C. Gold Nanoparticle-Based Miniaturized Nanomaterial Surface Energy Transfer Probe for Rapid and Ultrasensitive Detection of Mercury in Soil, Water, and Fish. *ACS Nano* **2007**, *1*, 208.
179. Jena, B. K.; Raj, C. R. Gold Nanoelectrode Ensembles for the Simultaneous Electrochemical Detection of Ultratrace Arsenic, Mercury, and Copper. *Anal. Chem.* **2008**, *80*, 4836.
180. Unger, A.; Kreiter, M. Analyzing the Performance of Plasmonic Resonators for Dielectric Sensing. *J. Phys. Chem. C* **2009**, *113*, 12243–1225.
181. Sönnischen, C.; Franzl, T.; Wilk, T.; von Plessen, G.; Feldmann, J.; Wilson, O.; Mulvaney, P. Drastic Reduction of Plasmon Damping in Gold Nanorods. *Phys. Rev. Lett.* **2002**, *88*, 077402.
182. Butet, J.; Russier-Antoine, I.; Jonin, C.; Lascoux, N.; Benichou, E.; Brevet, P.-F. Sensing with Multipolar Second Harmonic Generation from Spherical Metallic Nanoparticles. *Nano Lett.* **2012**, *12*, 1697–1701.
183. Östling, D.; Stampfli, P.; Benneman, K. H. Theory of Nonlinear Optical Properties of Small Metallic Spheres. *Z. Phys. D: At., Mol. Clusters* **1993**, *28*, 169–175.
184. Pavlyukh, Y.; Hubner, W. Nonlinear Mie Scattering from Spherical Particles. *Phys. Rev. B: Condens. Matter Mater. Phys.* **2004**, *70*, 245434.
185. de Beer, A. G. F.; Roke, S. Nonlinear Mie Theory for Second-Harmonic and Sum-Frequency Scattering. *Phys. Rev. B: Condens. Matter Mater. Phys.* **2007**, *75*, 245438.
186. Schürer, B.; Wunderlich, S.; Sauerbeck, C.; Peschel, U.; Peukert, W. Probing Colloidal Interfaces by Angle-Resolved Second Harmonic Light Scattering. *Phys. Rev. B: Condens. Matter Mater. Phys.* **2010**, *82*, 241404.
187. Gonella, G.; Dai, H.-L. Determination of Adsorption Geometry on Spherical Particles from Nonlinear Mie Theory Analysis of Surface Second Harmonic Generation. *Phys. Rev. B: Condens. Matter Mater. Phys.* **2011**, *84*, 121402(R).
188. Butet, J.; Russier-Antoine, I.; Jonin, C.; Lascoux, N.; Benichou, E.; Brevet, P.-F. Nonlinear Mie Theory for the Second Harmonic Generation in Metallic Nanoshells. *J. Opt. Soc. Am. B* **2012**, *29*, 2213–2221.
189. Capretti, A.; Forestiere, C.; Dal Negro, L.; Miano, G. Full-Wave Analytical Solution of Second-Harmonic Generation in Metal Nanospheres. *Plasmonics* **2014**, *9*, 151–166.
190. Morton, S. M.; Silverstein, D. W.; Jensen, L. Theoretical Studies of Plasmonics using Electronic Structure Methods. *Chem. Rev.* **2011**, *111*, 3962–3994.
191. Guo, C.; Rodriguez, G.; Taylor, A. J. Ultrafast Dynamics of Electron Thermalization in Gold. *Phys. Rev. Lett.* **2001**, *86*, 1638–1641.
192. Mukherjee, S.; Libisch, F.; Large, N.; Neumann, O.; Brown, L. V.; Cheng, J.; Lassiter, J. B.; Carter, E. A.; Nordlander, P.; Halas, N. J. Hot Electrons Do the Impossible: Plasmon-Induced Dissociation of H2 on Au. *Nano Lett.* **2013**, *13*, 240–247.
193. Kamat, P. V. Photovoltaics: Capturing Hot Electrons. *Nat. Chem.* **2010**, *2*, 809–810.
194. Brongersma, M. L.; Halas, N. J.; Nordlander, P. Plasmon-Induced Hot Carrier Science and Technology. *Nat. Nanotechnol.* **2015**, *10*, 25–34.
195. Yu, N.; Capasso, F. Flat Optics with Designer Metasurfaces. *Nat. Mater.* **2014**, *13*, 139–150.
196. Meinzer, N.; Barnes, W. L.; Hooper, I. R. Plasmonic Meta-Atoms and Metasurfaces. *Nat. Photonics* **2014**, *8*, 889–898.
197. Kildishev, A. V.; Boltasseva, A.; Shalaev, V. M. Planar Photonics with Metasurfaces. *Science* **2013**, *339*, 6125.
198. Minovich, A. E.; Miroshnichenko, A. E.; Bykov, A. Y.; Murzina, T. V.; Neshev, D. N.; Kivshar, Y. S. Functional and Nonlinear Optical Metasurfaces. *Laser Phot. Rev.* **2015**, *9*, 195–213.
199. Segal, N.; Keren-Zur, S.; Hendler, N.; Ellenbogen, T. Controlling Light with Metamaterials-Based Nonlinear Photonic Crystals. *Nat. Photonics* **2015**, *9*, 180–184.
200. Li, G.; Chen, S.; Pholchai, N.; Reineke, B.; Wong, P. W. H.; Pun, E. Y. B.; Cheah, K. W.; Zentgraf, T.; Zhang, S. Continuous Control of the Nonlinearity Phase for Harmonic Generations. *Nat. Mater.* **2015**, *14*, 607–612.
201. O'Brien, K.; Suchowski, H.; Rho, J.; Salandrino, A.; Boubacar, K.; Yin, X.; Zhang, X. Predicting Nonlinear Properties of Metamaterials from the Linear Response. *Nat. Mater.* **2015**, *14*, 379–383.
202. Suchowski, H.; O'Brien, K.; Wong, Z. J.; Salandrino, A.; Yin, X.; Zhang, X. Phase Mismatch—Free Nonlinear Propagation in Optical Zero-Index Materials. *Science* **2013**, *342*, 1223–1226.
203. Bao, Q.; Loh, K. P. Graphene Photonics, Plasmonics, and Broadband Optoelectronic Devices. *ACS Nano* **2012**, *6*, 3677–3694.
204. Garcia de Abajo, F. J. Graphene Plasmonics: Challenges and Opportunities. *ACS Photonics* **2014**, *1*, 135–152.
205. Dean, J. J.; van Driel, H. M. Second Harmonic Generation from Graphene and Graphitic Films. *Appl. Phys. Lett.* **2009**, *95*, 261910.

206. An, Y. Q.; Nelson, F.; Lee, J. U.; Diebold, A. C. Enhanced Optical Second-Harmonic Generation from the Current-Biased Graphene/SiO_2/Si(001) Structure. *Nano Lett.* **2013**, *13*, 2104–2109.
207. Smirnova, D. A.; Shadrivov, I. V.; Miroshnichenko, A. E.; Smirnov, A. I.; Kivshar, Y. S. Second-Harmonic Generation by a Graphene Nanoparticle. *Phys. Rev. B: Condens. Matter Mater. Phys.* **2014**, *90*, 035412.
208. Cox, J. D.; Garcia de Abajo, F. J. Electrically Tunable Nonlinear Plasmonics in Graphene Nanoislands. *Nat. Commun.* **2014**, *5*, 5725.